© 2020. Published by The Company of Biologists Ltd | Development (2020) 147, dev191155. doi:10.1242/dev.191155

RESEARCH ARTICLE

The membrane protein Raw regulates dendrite pruning via the secretory pathway

Menglong Rui[1,*], Shufeng Bu[1,2,*], Liang Yuh Chew[1,2,*], Qiwei Wang[1,2] and Fengwei Yu[1,2,3,‡]

ABSTRACT

Neuronal pruning is essential for proper wiring of the nervous systems in invertebrates and vertebrates. *Drosophila* ddaC sensory neurons selectively prune their larval dendrites to sculpt the nervous system during early metamorphosis. However, the molecular mechanisms underlying ddaC dendrite pruning remain elusive. Here, we identify an important and cell-autonomous role of the membrane protein Raw in dendrite pruning of ddaC neurons. Raw appears to regulate dendrite pruning via a novel mechanism, which is independent of JNK signaling. Importantly, we show that Raw promotes endocytosis and downregulation of the conserved L1-type cell-adhesion molecule Neuroglian (Nrg) prior to dendrite pruning. Moreover, Raw is required to modulate the secretory pathway by regulating the integrity of secretory organelles and efficient protein secretion. Mechanistically, Raw facilitates Nrg downregulation and dendrite pruning in part through regulation of the secretory pathway. Thus, this study reveals a JNK-independent role of Raw in regulating the secretory pathway and thereby promoting dendrite pruning.

KEY WORDS: Pruning, Raw, JNK signaling, Neuroglian, Axon, Dendrite

INTRODUCTION

During animal development, neurons often elaborate exuberant processes and connections at early stages. Selective elimination of their unnecessary processes without causing neuronal death, referred to as pruning, is essential for the maturation of the nervous systems at late stages (Luo and O'Leary, 2005; Riccomagno and Kolodkin, 2015; Schuldiner and Yaron, 2015). Developmental pruning widely occurs across the animal kingdom. In mammals, some neurons in the central and peripheral nervous systems can prune their unwanted or incorrect axons/dendrites to establish proper wiring of the nervous systems (O'Leary and Koester, 1993; Malun and Brunjes, 1996; Bagri et al., 2003; Riccomagno et al., 2012; Tapia et al., 2012). Aberrant pruning, which results in altered dendritic or axonal density in human brains, is often associated with neurological disorders, including autism spectrum disorder and schizophrenia (Tang et al., 2014; Sekar et al., 2016). Moreover, developmental pruning involves local degeneration and terminal retraction, morphologically resembling neurodegeneration associated with nerve injury and age-dependent neurodegenerative diseases. Thus, a comprehensive understanding of the underlying mechanisms of developmental pruning would provide important insights into pathogenesis of human brain disorders.

In the holometabolous insect *Drosophila*, many larval-born neurons in the central and peripheral nervous systems undergo stereotyped pruning to eliminate their larval dendrites and/or axons during metamorphosis (Truman, 1990). Dendrite pruning of class IV dendritic arborization sensory neurons (C4da) and axon pruning of mushroom body (MB) γ neurons are two appealing model systems for dissecting the molecular and cellular mechanisms of neuronal pruning (Yu and Schuldiner, 2014; Kanamori et al., 2015a). ddaC neurons, a subset of dorsal C4da neurons in the peripheral nervous system, elaborate long and branched dendrites at larval stages to nonredundantly cover the dorsal body surface and function as polymodal nociceptors (Jan and Jan, 2010). ddaC neurons prune away all their larval dendrites but keep their axons intact during the first day of metamorphosis (Kuo et al., 2005; Williams and Truman, 2005). At the proximal regions of ddaC dendrites, initial thinning and blebbing events take place at ∼4 h after puparium formation (APF), which leads to severing of the proximal dendrites, subsequent fragmentation and debris clearance (Fig. 1A). Like ddaC neurons, dorsal class I sensory neurons (ddaD and ddaE) also specifically prune their larval dendrites without affecting their axons (Williams and Truman, 2005).

In ddaC neurons, dendrite pruning initiates in response to a late larval pulse of the steroid hormone 20-hydroxyecdysone (ecdysone). Upon the binding of ecdysone, a heterodimer of ecdysone receptor complex, consisting of EcR-B1 and Ultraspiracle, acts together with two epigenetic factors Brahma and CREB-binding protein to trigger a downstream transcriptional cascade (Kirilly et al., 2009, 2011). The key transcription activator Sox14 and the negative growth regulator Headcase are induced by EcR-B1 (Kirilly et al., 2009; Loncle and Williams, 2012); Sox14, in turn, activates the expression of the actin disassembly factor Mical (Kirilly et al., 2009). The first cellular hallmark of dendrite pruning includes local thinning and blebbing of major dendrites at the proximal regions, which occurs as early as 4 h APF. Subsequently, major dendrites are severed between 5 and 8 h APF. Several known pathways that contribute to dendrite severing are: microtubule disassembly (Williams and Truman, 2005; Lee et al., 2009; Herzmann et al., 2017) and orientation (Herzmann et al., 2018; Wang et al., 2019; Rui et al., 2020; Tang et al., 2020), ubitquitin-proteosomal degradation (Kuo et al., 2005; Rumpf et al., 2011; Wong et al., 2013), endolysosomal degradation (Zhang et al., 2014; Krämer et al., 2019), secretory pathway (Wang et al., 2017, 2018), and local disassembly of plasma membrane (Kanamori et al., 2015b). Dendrite severing is induced by both global and local endocytosis. Via a Rab5/ESCRT-dependent endolysosomal degradation pathway, the conserved L1-type cell-adhesion molecule Neuroglian (Nrg) is internalized from the plasma membrane to early endosomes and drastically downregulated to induce the onset of dendrite pruning

[1]Temasek Life Sciences Laboratory, 1 Research Link, National University of Singapore, Singapore 117604. [2]Department of Biological Sciences, National University of Singapore, Singapore 117543. [3]NUS Graduate School for Integrative Sciences and Engineering, Centre for Life Sciences, Singapore 117456.
*These authors contributed equally to this work

‡Author for correspondence (fengwei@tll.org.sg)

F.Y., 0000-0003-0268-199X

Handling Editor: François Guillemot
Received 3 April 2020; Accepted 8 September 2020

Development (2020) 147, dev191155. doi:10.1242/dev.191155

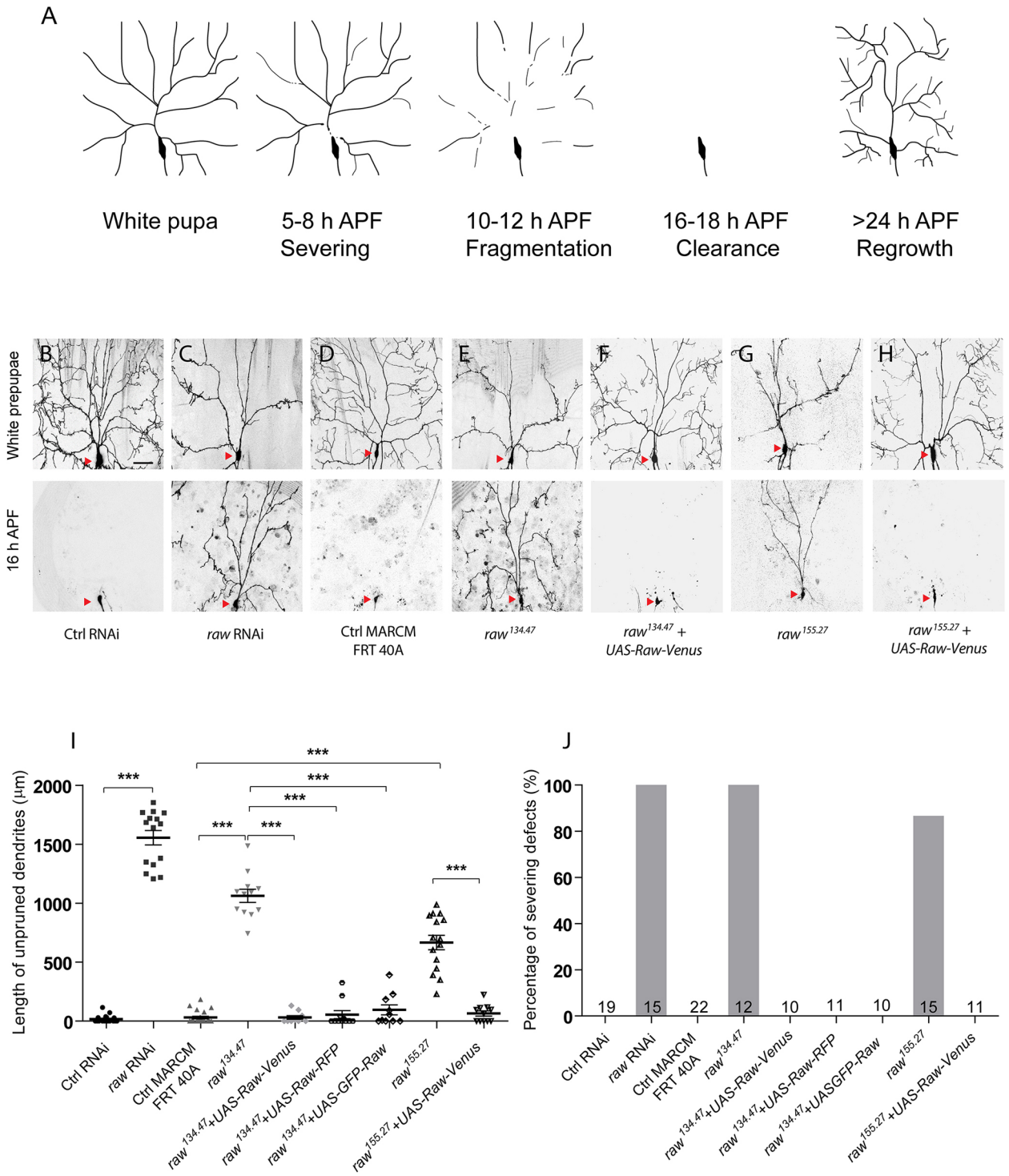

Fig. 1. Raw cell-autonomously regulates dendrite pruning of sensory neurons. (A) A schematic of dendrite pruning in ddaC sensory neurons. (B-H) Live confocal images of ddaC neurons expressing mCD8::GFP driven by *ppk-Gal4* at WP stage or 16 h APF. (B,D) Control neurons pruned away their larval dendrites at 16 h APF. *raw* RNAi and *raw* mutants ddaC neurons (C,E,G) displayed dendrite arborization defects at WP stage and pruning defects at 16 h APF. (F,H) Re-introduction of Raw-Venus rescued dendrite pruning defects in $raw^{134.47}$ and $raw^{155.27}$ clones. Red arrowheads indicate the ddaC somas. (I) Quantitative analysis of unpruned dendrite lengths. (J) Percentages of ddaC neurons showing severing defects. In I, data are mean±s.e.m. One-way ANOVA with Bonferroni's test and two-tailed Student's *t*-test were applied to determine statistical significance. ***P<0.001. The number of neurons (n) examined in each group is shown on the bars. Scale bar: 50 µm.

(Zhang et al., 2014). More recently, we also reported that Arf1/Sec71 and Yif1/Yip1 complexes regulate the secretory pathway and promote dendrite severing via the regulation of Nrg endolysosomal degradation (Wang et al., 2017, 2018). After severing, the dendrites are rapidly fragmented in a caspase-dependent manner (Williams et al., 2006), followed by phagocyte-mediated debris clearance (Williams and Truman, 2005; Han et al., 2014) at 16-18 h APF. Although considerable progress in the understanding of dendrite

Development (2020) 147, dev191155. doi:10.1242/dev.191155

pruning has been made in past years, our understanding of the molecular mechanisms is still far from complete.

To systematically understand the mechanisms of dendrite pruning, we previously conducted a genome-wide RNA interference (RNAi) screen to isolate novel regulators that are required for dendrite pruning (Kirilly et al., 2009). From this screen, we identified the membrane protein Raw as an important player of dendrite pruning. Raw was initially reported to govern embryonic dorsal closure, gonad morphogenesis, intestine regeneration and glial development via negatively regulating JNK signaling (Byars et al., 1999; Bates et al., 2008; Jemc et al., 2012; Zhou et al., 2017; Hans et al., 2018; Luong et al., 2018). It has been well documented that JNK signaling plays a crucial role in regulation of Wallerian degeneration: an axon degenerative process upon nerve injury (Miller et al., 2009; Xiong and Collins, 2012). Moreover, Raw has been shown to regulate degeneration of injured axons and dendrites via inhibiting Fos and Jun (Hao et al., 2019). Interestingly, in this study we show that Raw is required to promote dendrite pruning independently of JNK signaling. Rather, we demonstrate that Raw facilitates Nrg downregulation and dendrite pruning in part through the regulation of secretory pathway. Thus, we demonstrate a novel and JNK-independent role of Raw in regulating the secretory pathway during dendrite pruning.

RESULTS

Raw cell-autonomously regulates dendrite pruning of sensory neurons

In a large-scale RNAi screen, we isolated one RNAi line, v101255, that targets the *raw* gene. The expression of this RNAi line via the C4da-specific driver *ppk-Gal4* led to fully penetrant dendrite pruning defects in ddaC neurons at 16 h APF (Fig. 1C,J). These *raw* RNAi neurons retained an average of 1555 µm dendrites in the vicinity of their soma (Fig. 1I). In contrast, the neurons expressing the control RNAi line pruned away all their larval dendrites at the same time point (Fig. 1B,I,J). To further confirm the requirement of Raw for dendrite pruning, we used two previously published alleles, $raw^{134.47}$ and $raw^{155.27}$ (Jemc et al., 2012), and generated their mutant ddaC clones via mosaic analysis with a repressible cell marker (MARCM). Either $raw^{134.47}$ or $raw^{155.27}$ mutant clones exhibited consistent dendrite pruning defects with almost full penetrance at 16 h APF (Fig. 1E,G,J), in contrast to the control clones (Fig. 1D,J). Approximately 1063 and 666 µm dendrites remained in $raw^{134.47}$ or $raw^{155.27}$ mutant clones (Fig. 1I), respectively. Overexpression of Venus-tagged full-length Raw (Raw-Venus) fully rescued their dendrite pruning defects in $raw^{134.47}$ (Fig. 1F,I,J) and $raw^{155.27}$ (Fig. 1H-J) mutant neurons, respectively. The complete rescues were also achieved by the expression of RFP-tagged Raw (Raw-RFP) (Fig. S1A,I,J) as well as another previously published transgene expressing GFP-Raw (Fig. S1A,I,J). These rescue results demonstrate that the dendrite pruning defects in *raw* mutant neurons are caused by loss of *raw* function. Like ddaC neurons, class I ddaD/E neurons also undergo stereotyped dendrite pruning (Williams and Truman, 2005). While ddaD/E dendrites were specifically pruned in the control neurons by 19 h APF (Fig. S1B), all mutant ddaD/E neurons in which *raw* was knocked down via the $Gal4^{2\text{-}21}$ driver exhibited the dendrite pruning defects at the same time point (Fig. S1B). Thus, these data demonstrate an important role of Raw in regulating dendrite pruning in both types of sensory neurons during metamorphosis. In addition, we also observed that the number of primary and secondary dendrites was significantly reduced in *raw* RNAi (Fig. 1C, Fig. S1C) or *raw* mutant (Fig. 1E,G, Fig. S1C) neurons at WP stage. Overexpression of Raw-Venus significantly rescued the dendrite branching defects in *raw* mutant neurons (Fig. 1F,H, Fig. S1C). These data are consistent with the role of *raw* in regulate larval dendrite branching in class IV da neurons (Lee et al., 2015). To examine a specific function of Raw in dendrite pruning, we used the RU486-inducible gene-switch system (Osterwalder et al., 2001) to induce the expression of the *raw* RNAi construct at the larval stage. RU486-mediated knockdown of *raw* led to dendrite pruning defects in 42% of ddaC neurons (Fig. S1D). An average of 960 µm dendrites persisted in these RU486-inducible mutant neurons (Fig. S1D). Taken together, Raw plays a cell-autonomous role in dendrite pruning of sensory neurons during metamorphosis, in addition to its role in larval dendrite arborization.

The first Raw repeat, the putative transmembrane domain and the C-terminal region are important for Raw function in dendrite pruning

Raw protein contains two Raw repeats: a putative transmembrane (TM) domain; and a short carboxy-terminal (C-terminal) region (Fig. 2A) that shares some homology with the nematode OLRN-1 (Bauer Huang et al., 2007). To determine which domain is required for Raw function during dendrite pruning, we generated a series of transgenes expressing several Raw deletions and performed the rescue experiments in the $raw^{134.47}$ mutant background. The expression of full-length Raw fully rescued the dendrite pruning and arborization defects in $raw^{134.47}$ mutant clones (Fig. 2C,H, Fig. S2A), compared with the $raw^{134.47}$ neurons alone (Fig. 2B, Fig. S2A). Either $Raw^{\Delta R1}$, which deletes the first repeat, or $Raw^{\Delta C\text{-}ter}$, which deletes the C-terminal region, was unable to rescue the dendrite pruning and arborization defects in $raw^{134.47}$ mutant clones (Fig. 2D,G,H, Fig. S2A). However, the expression of $Raw^{\Delta R2}$, which deletes the second repeat, largely rescued the dendrite pruning and branching defects in $raw^{134.47}$ mutant neurons (Fig. 2E, H, Fig. S2A), indicating that the first repeat but not the second one is required for Raw function. These results are similar to those in its nematode homolog OLRN-1, which also shows that the first Raw repeat and the C-terminal region are important for its function in *C. elegans* (Bauer Huang et al., 2007). Importantly, the expression of the $Raw^{\Delta TM}$ variant that lacks the putative TM domain failed to rescue the $raw^{134.47}$ phenotypes (Fig. 2F,H, Fig. S2A), suggesting that potential membrane targeting of Raw is important for regulating dendrite pruning and arborization. As a control, overexpression of the Raw variants did not disturb normal dendrite pruning in wild-type ddaC neurons (Fig. S2B). Thus, the structure-function analysis indicates the requirement of the first repeat, the putative TM domain and the C-terminal region for Raw function in dendrite pruning. This result also supports the notion that Raw likely associates with the membranes to exert its function in dendrite pruning of ddaC neurons.

Raw regulates dendrite pruning independently of JNK signaling

We next attempted to understand the mechanism whereby Raw regulates dendrite pruning. Raw negatively regulates JNK signaling during development (Byars et al., 1999; Bates et al., 2008). To test a possible role of *raw* in regulating JNK signaling in ddaC neurons, we made use of the JNK reporter *puc-lacZ* to examine the expression of the target gene *puckered* and indicate the level of JNK signaling. Similar to the control neurons (Fig. 3A,E), knockdown of *raw* in ddaC neurons did not significantly alter the expression level of the *puc-lacZ* reporter at the wandering 3rd instar larval (wL3) stage (Fig. 3B,E), consistent with that reported in a previous study

Development (2020) 147, dev191155. doi:10.1242/dev.191155

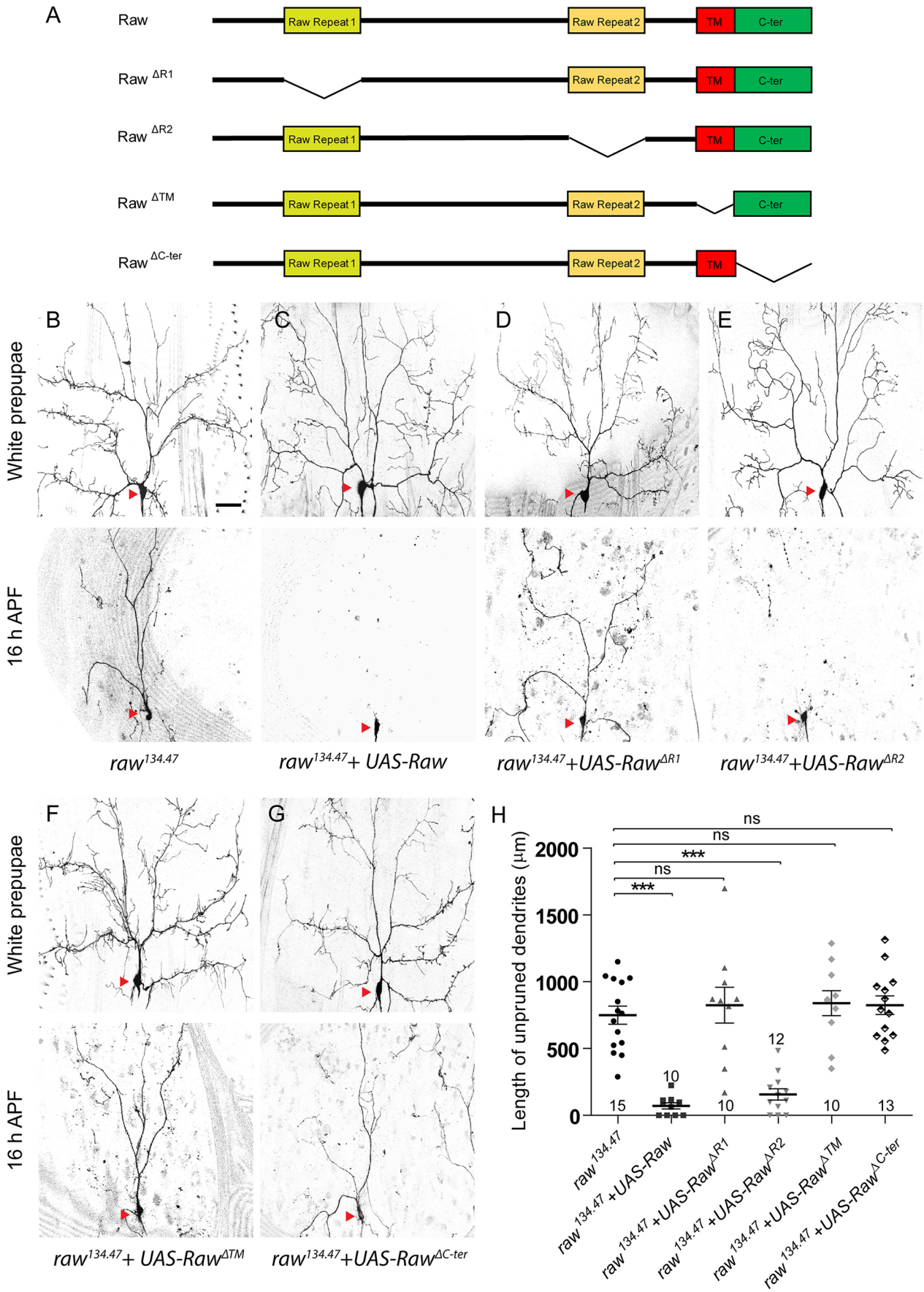

Fig. 2. See next page for legend.

Development (2020) 147, dev191155. doi:10.1242/dev.191155

Fig. 2. The first Raw repeat, the putative transmembrane domain and the C-terminal region are important for its function in dendrite pruning. (A) A schematic diagram showing the full-length Raw protein with different domains, and various truncated Raw proteins. (B-G) Live confocal images of ddaC neurons expressing mCD8::GFP driven by *ppk-Gal4* at WP stage or 16 h APF. $raw^{134.47}$ mutant ddaC clones (B) displayed the pruning defects at 16 h APF. (C-G) The rescue effect of Raw, $Raw^{\Delta R1}$, $Raw^{\Delta R2}$, $Raw^{\Delta TM}$ or $Raw^{\Delta C\text{-}ter}$ on the $raw^{134.47}$ phenotypes. Red arrowheads indicate the ddaC somas. (H) Quantitative analysis of unpruned dendrite lengths (data are mean±s.e.m.). One-way ANOVA with Bonferroni's test was applied to determine statistical significance. ns, not significant; ***P<0.001. The number of neurons (n) examined in each group is shown on the bars. Scale bar: 50 µm.

(Lee et al., 2015). Interestingly, the *puc-lacZ* expression levels significantly increased 2.4-fold at white prepupal (WP) stage (Fig. 3D,E), compared with the control RNAi neurons (Fig. 3C,E). Thus, JNK signaling appeared to be hyperactivated in *raw* RNAi ddaC neurons before the onset of dendrite pruning, which mimicked that in *raw* RNAi motor neurons (Hao et al., 2019). To investigate whether the elevated JNK activity in *raw* RNAi neurons contributes to the dendrite pruning defects, we expressed JNK^{DN}, the dominant-negative form of JNK that is encoded by *bsk* in *Drosophila*, in either *raw* RNAi or $raw^{155.27}$ mutant ddaC neurons. JNK^{DN} expression, which was shown to fully inhibit the JNK signaling in motor neurons (Xiong et al., 2010), also significantly suppress the *puc-LacZ* expression levels in wild-type ddaC neurons at WP stage (Fig. S3A). The expression of either JNK^{DN} transgenes, via one copy of *ppk-Gal4* driver, did not rescue the dendrite pruning defects in *raw* RNAi (Fig. 3F-H,L,M) and $raw^{155.27}$ mutant neurons (Fig. 3I-K-M). As a control, JNK^{DN} overexpression blocked the upregulation of *puc-LacZ* expression in *raw* RNAi ddaC neurons at WP stage (Fig. S3B), indicating that this dominant-negative construct is effective in ddaC sensory neurons. Similarly, the treatment with GNE-3511, a potent DLK inhibitor that significantly attenuated the JNK activity (Fig. S4A) (Feng et al., 2019), did not rescue the pruning defects in *raw* RNAi neurons (Fig. S4B). JNK signaling functions through its downstream Activator Protein 1 (AP-1) complex, which is composed of Jun and Fos transcription factors. Overexpression of either dominant-negative constructs (Fos^{DN} or Jun^{DN}), via one copy of the *ppk-Gal4* driver, also did not rescue the pruning defects in *raw* RNAi neurons (Fig. S5A), although Fos^{DN} or Jun^{DN} expression was reported to rescue the injury-induced axon degeneration phenotypes in *raw* mutant motor neurons (Hao et al., 2019). Jun^{DN} or Fos^{DN} expression was able to significantly suppress the *puc-LacZ* expression in both wild-type (Fig. S3A) and *raw* RNAi (Fig. S3B) ddaC neurons at WP stage, suggesting that both constructs effectively attenuate the JNK activity. Moreover, high-level expression of JNK^{DN}, Jun^{DN} or Fos^{DN}, via two copies of *ppk-Gal4* driver, failed to rescue the dendrite pruning defects in *raw* RNAi neurons (Fig. S5B). In addition, overexpression of wild-type JNK, Fos or Jun alone did not inhibit dendrite pruning in wild-type ddaC neurons (Fig. S6A). Either JNK or Fos expression augmented the JNK activity, as indicated by elevated *puc-LacZ* levels (Fig. S6B). Taken together, these data indicate that Raw is unlikely to regulate dendrite pruning by suppressing JNK signaling, which contrasts with its role in injury-induced axon degeneration in motor neurons.

Raw has previously been reported to distribute in both membranes and cytoplasm; it could potentially act as a cell-adhesion molecule to govern terminal dendrite branching of C4da neurons via activating the Tricornered (Trc)/Furry (Fry) pathway (Lee et al., 2015). However, we did not observe any dendrite pruning defect in either trc^{1} or fry^{1} mutant ddaC clones (Fig. S5C), suggesting that Raw may not require Trc or Fry during dendrite pruning. Our previous study also indicates that the cell-adhesion molecule Neuroglian is degraded via the endolysosomal degradation machinery before the onset of dendrite pruning (Zhang et al., 2014). If Raw functions as a cell-adhesion molecule to regulate dendrite pruning, one might consider whether Raw, like Nrg, also undergoes the Rab5/ESCRT-mediated endolysosomal degradation prior to dendrite pruning. Nrg robustly accumulated on enlarged endosomes and colocalized with the endosomal marker Avalanche (Avl, also known as Syntaxin 7) in $Rab5^{DN}$ or $Vps4^{DN}$ mutant neurons (Fig. S7A) (Zhang et al., 2014). In contrast, RFP-tagged Raw exhibited no accumulation in $Rab5^{DN}$ or $Vps4^{DN}$ mutant neurons (Fig. S7B). Moreover, Nrg was redistributed from the plasma membrane (WP stage) to the GFP-2XFYVE-positive early endosomes at 6 h APF in ddaC neurons (Fig. S7C) (Zhang et al., 2014). Unlike Nrg, RFP-Raw did not colocalize with these endosomes at wL3 and 6 h APF stages (Fig. S7D). Finally, Raw overexpression did not inhibit dendrite pruning (Fig. S2B), in contrast to the dendrite pruning defects in Nrg-overexpressing neurons (Zhang et al., 2014). Thus, these data indicate that Raw is unlikely to undergo endolysosomal degradation before the onset of dendrite pruning. In addition, dendritic microtubule levels and orientation, as detected by the microtubule-associated protein Futsch (22C10) and EB1-GFP comet directionality, respectively, were not affected in the dendrites of *raw* RNAi ddaC neurons (Fig. S7E,F), suggesting that Raw is dispensable for microtubule mass and polarity in the dendrites. Taken together, Raw is unlikely to regulate dendrite pruning via JNK signaling, Trc/Fry pathway or endolysosomal degradation.

Raw is required for endocytosis and downregulation of Nrg prior to dendrite pruning

In an attempt to examine Nrg distribution in *raw* mutant neurons, we consistently observed its robust accumulation in both *raw* RNAi and mutant neurons. Nrg, as detected by the BP104 antibody, was localized in the soma, dendrites and axons in the control ddaC neurons at wL3 stage (Fig. 4A). Importantly, RNAi knockdown of *raw* led to a significant increase in the Nrg expression level in ddaC neurons at the same stage (Fig. 4B,E), similar to $Rab5^{DN}$ overexpression (Fig. 4M) or *arf1* knockdown (Fig. S8A,D). More strikingly, Nrg levels were elevated over threefold in *raw* RNAi neurons at 6 h APF (Fig. 4D,F), compared with those in the controls (Fig. 4C,F). Nrg RNAi knockdown significantly eliminated the Nrg signals in *raw* RNAi ddaC neurons (Fig. S8B,D), further confirming that Nrg protein levels are elevated upon *raw* knockdown. Moreover, we also observed a similar accumulation of Nrg in $raw^{134.47}$ or $raw^{155.27}$ neurons at wL3 stage (Fig. 4H,I,J; wild type, Fig. 4G). Interestingly, the levels of another transmembrane protein Ppk26, functioning as a DEG/ENaC ion channel in C4da neurons, remained unchanged in *raw* RNAi neurons (Fig. S9A). Overexpression of JNK or Fos, which led to elevated *puc-LacZ* expression (Fig. S6B), showed no aberrant Nrg accumulation (Fig. S6C), suggesting that hyperactivated JNK signaling in *raw* mutant neurons is not responsible for Nrg accumulation. In addition, overexpression of Raw did not disturb the expression level and pattern of Nrg in ddaC neurons (Fig. S8C,D); no physical interaction between Raw and Nrg was detected, as Raw-Venus was not able to pull down endogenous Nrg in the co-immunoprecipitation experiments using the protein extracts from the adult brains overexpressing Raw-Venus (Fig. S8E). Thus, these control experiments suggest that Raw may indirectly regulate Nrg protein stability.

Development (2020) 147, dev191155. doi:10.1242/dev.191155

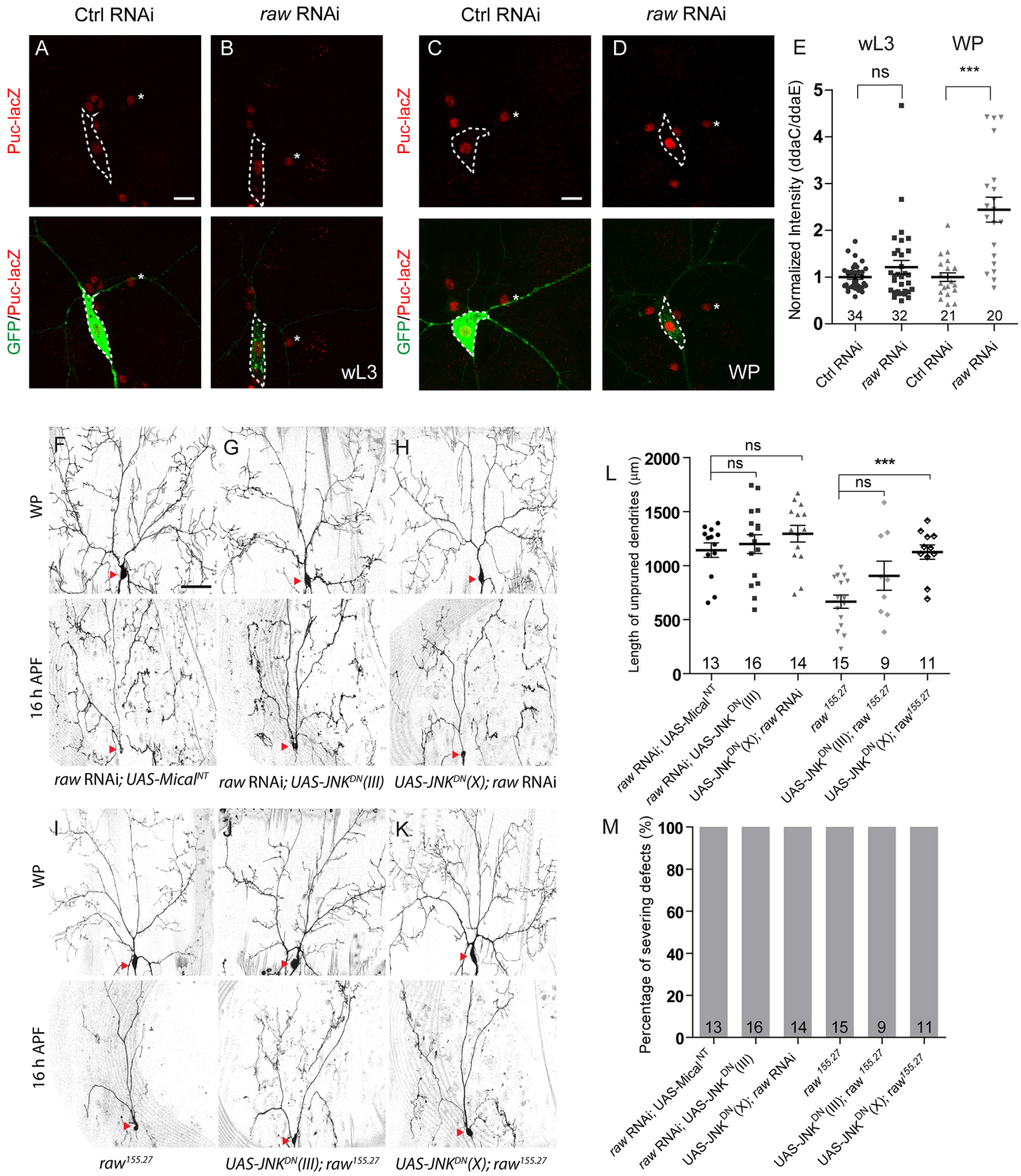

Fig. 3. Raw regulates dendrite pruning independently of JNK signaling. (A-D) Confocal images of control RNAi (A,C) and *raw* RNAi (B,D) ddaC neurons that were immunostained for LacZ at wL3 and WP stages. ddaC somas are outlined with dashed lines, ddaE somas are indicated with asterisks. ddaC neurons were identified by *ppk-Gal4*-driven mCD8::GFP (green channel) expression. (E) Quantitative analysis of normalized *puc-lacZ* fluorescence intensities in ddaC somas. (F-K) Live confocal images of ddaC neurons expressing mCD8::GFP driven by *ppk-Gal4* at WP or 16 h APF stages. *raw* RNAi and $raw^{134.47}$ mutant ddaC neurons (F,I) displayed the pruning defects at 16 h APF. (G,H,J,K) The expression of JNK^{DN} (III) and JNK^{DN} (X) did not rescue the dendrite pruning defects in *raw* RNAi or $raw^{155.27}$ mutant ddaC clones. Red arrowheads indicate the ddaC somas. (L) Quantitative analysis of unpruned dendrite lengths. (M) Percentages of ddaC neurons showing severing defects. In E,L, data are mean±s.e.m. One-way ANOVA with Bonferroni's test and a two-tailed Student's *t*-test were applied to determine statistical significance. ns, not significant; ***P<0.001. The number of neurons (n) examined in each group is shown on the bars. Scale bars: 10 μm in A,C; 50 μm in F.

Development (2020) 147, dev191155. doi:10.1242/dev.191155

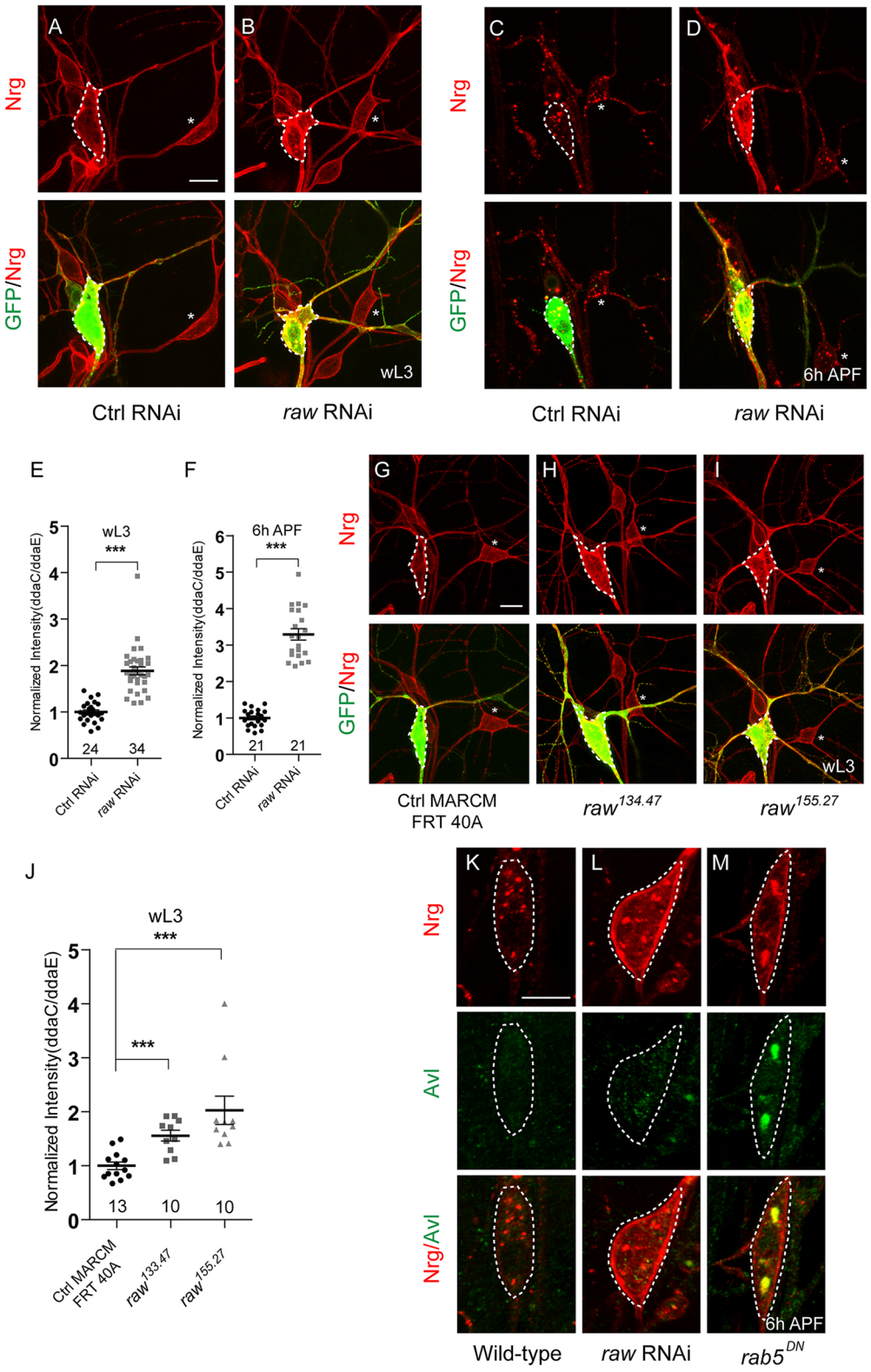

Fig. 4. Raw is required for downregulation of Nrg prior to dendrite pruning. (A-D) Confocal images of control RNAi (A,C) and *raw* RNAi (B,D) ddaC neurons that were immunostained for Nrg at wL3 and 6 h APF stages. (E,F) Quantitative analysis of normalized Nrg fluorescence intensities in ddaC somas. (G-I) Confocal images of Ctrl MARCM (G), $raw^{134.47}$ MARCM (H) and $raw^{155.27}$ MARCM (I) ddaC clones that were immunostained for Nrg at wL3 stage. ddaC somas are outlined with dashed lines, ddaE somas are indicated with asterisks. ddaC neurons were identified by *ppk-Gal4*-driven mCD8::GFP (green channel) expression. (J) Quantitative analysis of normalized Nrg fluorescence intensities in ddaC somas. (K-M) Confocal images of wild-type (K), *raw* RNAi (L) and $rab5^{DN}$ (M) ddaC neurons that were immunostained for Nrg at 6 h APF. ddaC somas are outlined with dashed lines. In E,F,J, data are mean±s.e.m. One-way ANOVA with Bonferroni's test and a two-tailed Student's *t*-test were applied to determine statistical significance. ***P<0.001. The number of neurons (n) examined in each group is shown on the bars. Scale bars: 10 µm.

Interestingly, the distribution pattern of Nrg in *raw* RNAi or mutant neurons (Fig. 4B,D) is distinct from that in $Rab5^{DN}$-expressing neurons (Fig. S7A). In wild-type ddaC neurons, Nrg protein was drastically redistributed to punctate structures and colocalized with the early endosomal marker GFP-2XEGFP at 6 h APF (Fig. 4K, Fig. S7C), suggesting active endocytosis and degradation of Nrg prior to dendrite pruning (Zhang et al., 2014). However, elevated Nrg was primarily localized on the cortex of *raw* RNAi neurons and exhibited several small punctate structures in the cytoplasm (Fig. 4L), suggesting that Nrg endocytosis is primarily inhibited in these mutant neurons. This phenotype contrasts with the $Rab5^{DN}$ phenotype in which Nrg was present at higher levels on two or three enlarged endosomes positive for Avl (Fig. 4M, Fig. S7A) (Zhang et al., 2014). Raw knockdown did not lead to accumulation of

Development (2020) 147, dev191155. doi:10.1242/dev.191155

ubiquitylated protein aggregates (Fig. S8F) and enlarged Avl-positive endosomes (Fig. 4L), in contrast to those in Rab5^{DN} (Fig. 4M, Fig. S8F) or Vsp4^{DN} expression (Fig. S7A) (Zhang et al., 2014). These data suggest that, unlike Rab5 and Vps4, Raw may indirectly regulate the endolysosomal degradation of Nrg. Thus, Raw promotes endolysosomal degradation of Nrg prior to dendrite pruning.

Raw is required for ER/Golgi integrity and protein secretion in ddaC neurons

The phenotypes in *raw* RNAi or mutant neurons, such as elevated Nrg levels and no ubiquitylated protein aggregates, are reminiscent of those observed in mutant neurons depleting the regulators of secretory pathway, including Arf1/Sec71, Yif1/Yip1 and Rab1 (Wang et al., 2017, 2018). This prompted us to investigate a possible role for Raw in regulating the secretory pathway during dendrite pruning. To this end, we first assessed whether Raw is required for proper localization of endoplasmic reticulum (ER) markers or regulators. In the control neurons, Sec31-mCherry, an ER exit site marker, was localized as many discrete punctate structures in the soma (Fig. 5A). Strikingly, these Sec31-mCherry puncta were almost lost when *raw* was knocked down in ddaC neurons (Fig. 5A). Likewise, the punctate signals of endogenous Rab1, an important regulator of the ER-to-Golgi transport, significantly decreased in intensity in *raw* RNAi neurons (Fig. 5B), compared with its bright puncta in the control neurons (Fig. 5B). Next, we tested several Golgi markers and secretory regulators. Both the endogenous *cis*-Golgi marker GM130 and a *trans*-Golgi marker galactosyltransferase-RFP (GalT-RFP) were strongly reduced in total level in the soma of *raw* RNAi neurons (Fig. 5C,D), compared with their bright punctate signals in the controls (Fig. 5C,D). Dendritic GalT-RFP signals were much dimmer in intensity in *raw* RNAi neurons than those in the controls (Fig. S10A). Moreover, *raw* knockdown also led to significant reductions in the fluorescence intensity of endogenous Arf1 and Sec71 (Fig. 5E,F), two secretory regulators required for dendrite pruning (Wang et al., 2017). In addition to the average reduction in total intensity, we often observed more individual puncta with reduced size and faint intensity in *raw* RNAi neurons. By contrast, overexpression of Raw did not interfere with the punctate localizations of Rab1 and GM130 (Fig. S10B). In addition, neither JNK nor Fos expression impaired the expression and distribution of Rab1 (Fig. S6D) and GM130 (Fig. S6E) in ddaC neurons. Interestingly, RNAi knockdown of *raw*, via the epidermal driver *A58-Gal4*, did not lead to any defect in the expression of GM130 in epidermal cells (Fig. S9B). Using a *raw-GFP* enhancer-trap line (*raw*^{MI07292}) (Zhou et al., 2017), we observed that Raw was predominantly expressed in sensory neurons but undetectable in the epidermal cells (Fig. S9C), suggesting a neuron-specific role for Raw. Collectively, these data suggest that Raw is required for the integrity of ER/Golgi apparatus in ddaC neurons.

To examine whether Raw regulates the secretion of the transmembrane protein to the cell surface, we conducted a trafficking assay for mCD8-GFP and measured the levels of extracellular mCD8 epitope under detergent-free conditions. In the control RNAi neurons, the extracellular mCD8 signals were strongly present on the dendrites using the anti-mCD8 antibody in the absence of the detergent (Fig. S10C). Importantly, mCD8 signals significantly decreased in the dendrites of *raw* RNAi neurons under detergent-free conditions (Fig. S10C). Overall GFP fluorescence, which represents both cell-surface and internal pools of the protein, was comparable between the control and *raw* RNAi neurons (Fig. S10C). Thus, the trafficking assay suggests that Raw is required for protein secretion in ddaC neurons.

Next, we attempted to examine whether Raw localizes on ER or Golgi as a component to govern their integrity. Several anti-Raw antibodies were generated but none of them was able to detect the endogenous protein in immunostaining assays. We therefore used the Raw-RFP transgene to investigate its subcellular distribution. Raw-RFP expression fully rescued the dendrite pruning defects in *raw*$^{134.47}$ mutant ddaC clones (Fig. 1I,J, Fig. S1A), suggesting that Raw-RFP can functionally substitute for the endogenous Raw protein. Under the control of the *ppk-Gal4* driver, Raw-RFP exhibited many discrete punctate structures (Fig. S7B,D). These Raw-RFP signals were largely eliminated by the expression of the *raw* RNAi line (Fig. S10D), indicating that these punctate signals indeed represent the Raw-RFP protein. To understand the identity of these punctate structures, we co-expressed Raw-RFP with various ER/Golgi markers. We observed that Raw-RFP signals often colocalized with some of the KDEL-GFP-positive puncta (Fig. 5G), suggesting that Raw-RFP can localize on ER compartment. Raw-RFP signals localized adjacent to some puncta positive for the *trans*-Golgi marker GalT-GFP (Fig. 5H). These data suggest that these Raw-RFP puncta might be the vesicular subcompartment of ER or Golgi. We observed no detectable interaction between Raw and Arf1 in the co-immunoprecipitation assays using adult fly brains expressing Raw-Venus (Fig. S10E). Thus, our data suggest that Raw is unlikely a core component of ER/Golgi organelles but might regulate some vesicular subcompartment of the secretory pathway. Taken together, our observations suggest that Raw is required to regulate the integrity of ER/Golgi compartments and protein secretion in ddaC neurons.

Raw regulates Nrg downregulation and dendrite pruning at least in part via the secretory pathway

We have shown that Raw is required for both Nrg downregulation (Fig. 4) and the integrity of secretory compartments (Fig. 5). We further examined whether an altered secretory pathway contributes to abnormal Nrg accumulations and dendrite pruning in *raw* RNAi neurons. *raw* knockdown led to a significant increase in Nrg levels in ddaC neurons (Fig. 4B,D), compared with those in the wild type (Fig. 4A,C). Given impaired secretory pathway in *raw* RNAi neurons, we overexpressed the constitutive active forms of Rab1 (Rab1^{CA}) and the Arf1GEF Sec71 to enhance the secretory pathway in *raw* RNAi neurons. Interestingly, overexpression of Rab1^{CA} led to a significant rescue in Nrg levels in *raw* RNAi mutant neurons at wL3 stage (Fig. 6C,E). Likewise, overexpression of Sec71, which activates Arf1 function as its guanine nucleotide exchange factor (Wang et al., 2017), also significantly suppressed the Nrg expression to the normal level in *raw* RNAi neurons at wL3 stage (Fig. 6D,E). Moreover, the Nrg levels in *raw* RNAi neurons were significantly suppressed by Rab1^{CA} (Fig. 6H,J) or Sec71 overexpression (Fig. 6I,J) at 6 h APF, a stage before the onset of dendrite severing. As controls, the Nrg levels were not suppressed when the constitutive active forms of Rab11 or Arf6, regulators of endocytic pathways, were overexpressed in *raw* RNAi neurons at wL3 and 6 h APF stages (Fig. S11A-D). Thus, these rescue data suggest that abnormal Nrg accumulation in *raw* RNAi or mutant neurons is caused partially by an impaired secretory pathway.

Moreover, overexpression of Rab1^{CA} (Fig. 7B,D) or Sec71 (Fig. 7C,D) significantly suppressed the dendrite pruning defects in *raw* RNAi neurons, compared with the control (Fig. 7A,D). However, Rab1^{CA} or Sec71 overexpression did not rescue the dendrite length defects in *raw* RNAi neurons at WP stage (Fig. S12A), suggesting a specific effect of Rab1^{CA} and Sec71 on dendrite pruning in the mutant neurons. As controls, overexpression of Rab1^{CA} or Sec71 in

Development (2020) 147, dev191155. doi:10.1242/dev.191155

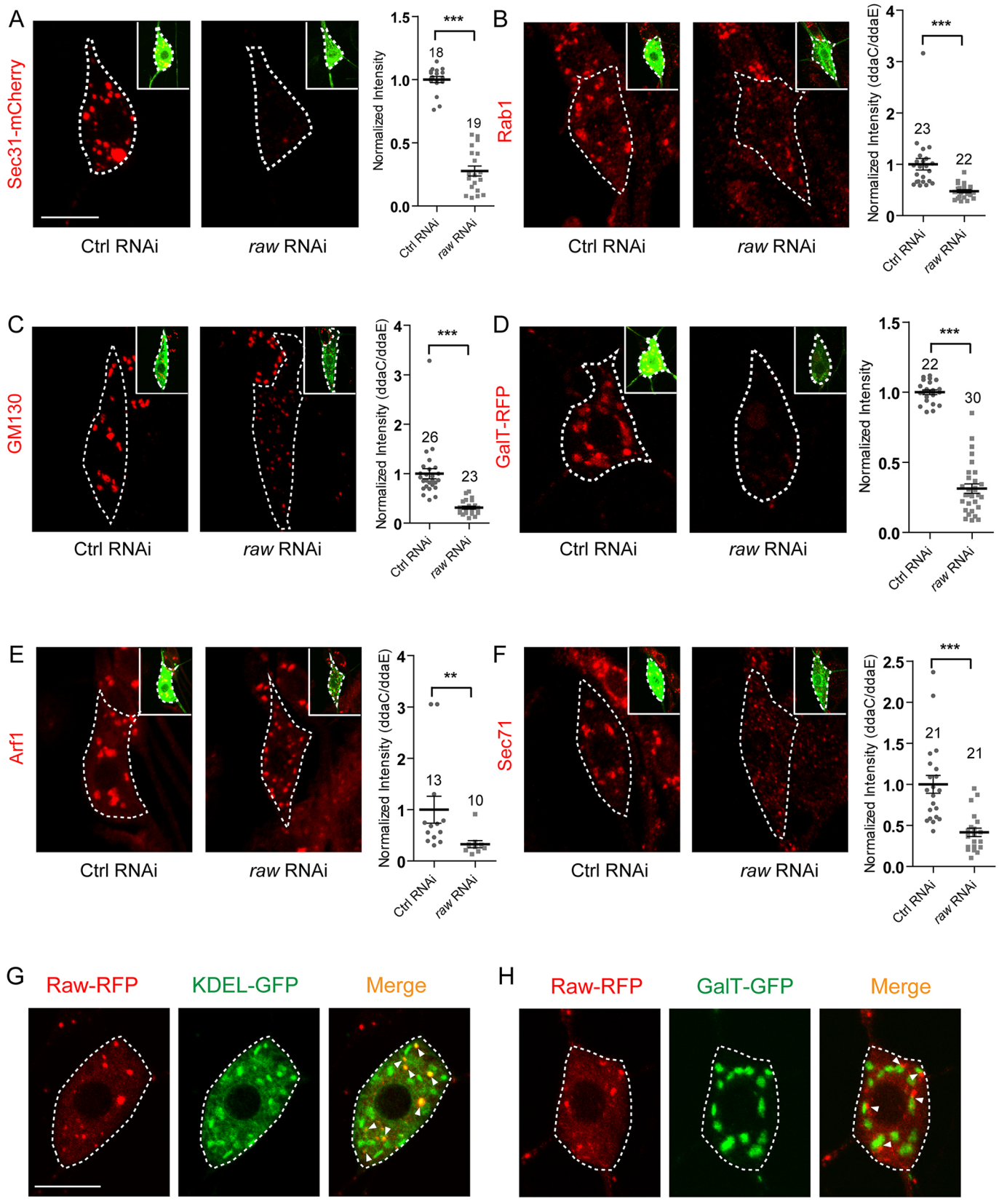

Fig. 5. Raw is required for the integrity of ER and Golgi compartments in ddaC sensory neurons. (A-F) Confocal images of Ctrl RNAi and *raw* RNAi ddaC neurons that were labelled for Sec31-mCherry, Rab1, GM130, GalT-RFP, Arf1 and Sec71 at wL3 stage. ddaC somas are outlined with dashed lines. ddaC neurons were identified by *ppk-Gal4*-driven mCD8::GFP (green channel) expression (insets). Quantitative analysis of normalized fluorescence intensities in ddaC somas (right panels). (G,H) Confocal live images of ddaC neurons that were labelled for Raw-RFP and KDEL-GFP, as well as Raw-RFP and GalT-GFP. In A-F, data are mean±s.e.m. Two-tailed Student's *t*-test was applied to determine statistical significance. ***P*<0.01, ****P*<0.001. The number of neurons (*n*) examined in each group is shown on the bars. Scale bars: 10 µm.

Development (2020) 147, dev191155. doi:10.1242/dev.191155

the control RNAi neurons did not cause any dendrite pruning defects at 16 h APF (Fig. S12B). Overexpression of Rab11^{CA} or Arf6^{CA}, which did not exhibit any dendrite pruning defects in the control RNAi neurons (Fig. S12B), neither suppressed nor enhanced the dendrite pruning defects associated with Raw knockdown (Fig. S12C). Thus, these experiments suggest that the dendrite pruning defects and aberrant Nrg accumulation in *raw* mutant neurons are caused partly by impaired secretory pathway. To further confirm whether the dendrite pruning defect in *raw* mutant neurons is indeed attributable to aberrant Nrg accumulation, we knocked down Nrg in *raw* RNAi ddaC neurons. Indeed, the expression of two independent *nrg* RNAi transgenes, both of which efficiently knocked down Nrg protein (Fig. S8B), significantly suppressed the dendrite pruning defects in *raw* RNAi ddaC neurons (Fig. 7F-H).

Taken together, our data suggest that Raw regulates Nrg downregulation and dendrite pruning at least partly through the secretory pathway. To the best of our knowledge, this is the first study showing a functional link between Raw and the secretory pathway.

DISCUSSION

Neuronal pruning is a conserved mechanism used to refine the mature nervous system during animal development (Riccomagno

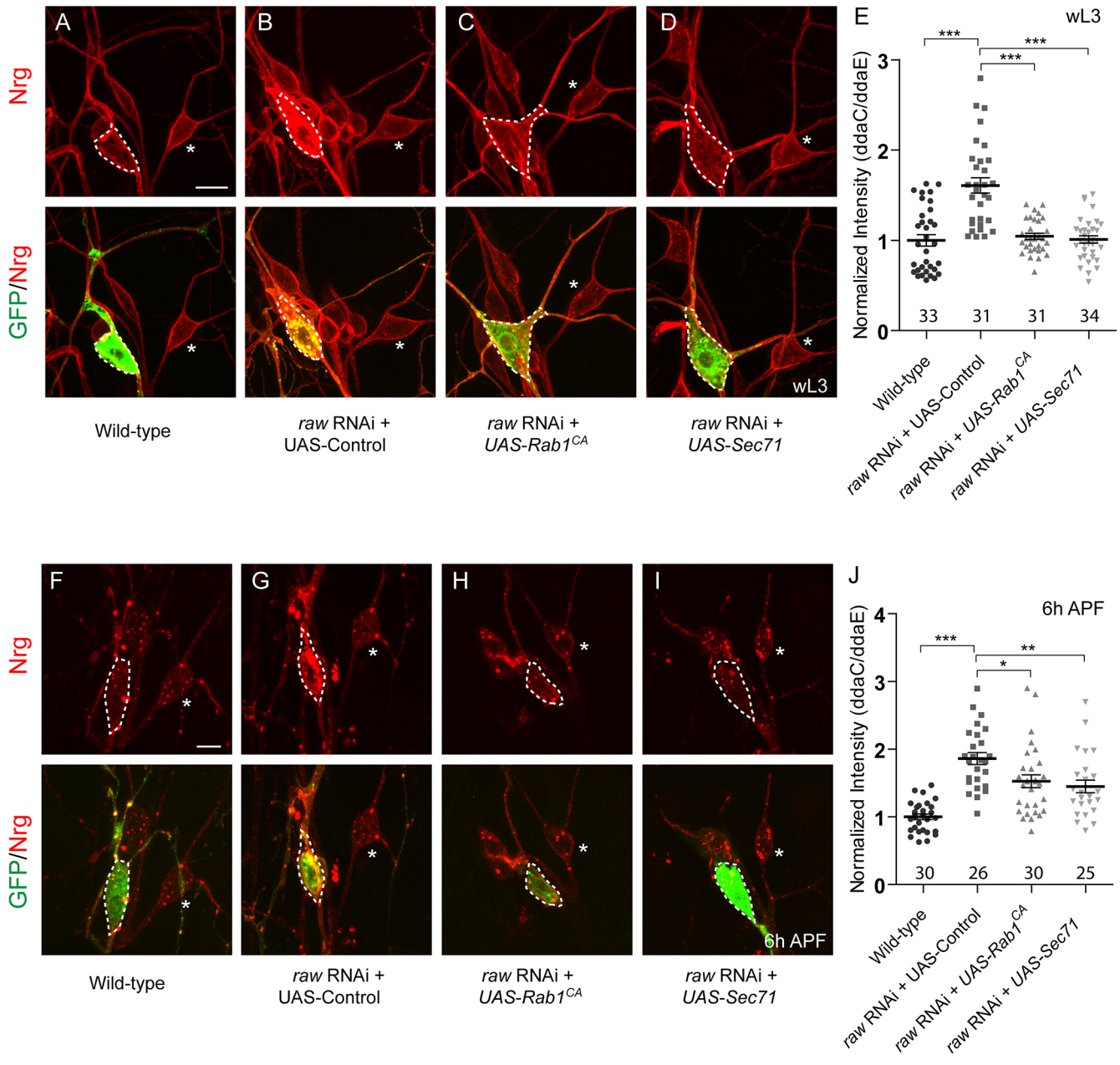

Fig. 6. Raw regulates Nrg downregulation partly via the secretory pathway. (A-D,F-I) Confocal images of wild-type (A,F), *raw* RNAi+*UAS-Control* (B,G), *raw* RNAi+*UAS-Rab1*^{CA} (C,H) and *raw* RNAi+*UAS-Sec71* (D,I) ddaC neurons immunostained for Nrg at wL3 and 6 h APF stages. ddaC somas are outlined with dashed lines, ddaE somas are indicated with asterisks. ddaC neurons were identified by *ppk-Gal4*-driven mCD8::GFP (green channel) expression. (E,J) Quantitative analysis of normalized Nrg fluorescence intensities in ddaC somas. In E,J, data are mean±s.e.m. One-way ANOVA with Bonferroni's test was applied to determine statistical significance. ns, not significant. **P*<0.05, ***P*<0.01, ****P*<0.001. The number of neurons (*n*) examined in each group is shown on the bars. Scale bars: 10 µm.

Development (2020) 147, dev191155. doi:10.1242/dev.191155

and Kolodkin, 2015; Schuldiner and Yaron, 2015). Despite the considerable progress made in previous years, our understanding of the molecular mechanisms is still incomplete. Here, we have identified the membrane protein Raw as a new regulator of dendrite pruning in our genome-wide RNAi screen. We found that Raw does not regulate dendrite pruning by inhibiting the JNK signaling. Instead, Raw regulates the secretory pathway to promote endolysosomal degradation of Nrg during dendrite pruning. Thus, this study reveals a novel and JNK-independent role of Raw in regulating the secretory pathway during dendrite pruning.

Raw regulates dendrite pruning in a JNK-independent manner

Numerous studies have reported an antagonism between Raw and JNK signaling in regulating various developmental processes in *Drosophila*, including embryonic dorsal closure, gonad morphogenesis, intestine regeneration and glial development (Byars et al., 1999; Bates et al., 2008; Jemc et al., 2012; Hans et al., 2018; Luong et al., 2018). Loss of *raw* function leads to elevated JNK activity, which contributes to the defects in these developmental processes. JNK signaling has been well documented to play vital roles in multiple neuronal events, including axon/dendrite growth, axon degeneration and regeneration in both development and diseases (Coffey, 2014). Growing studies have highlighted a key role of JNK signaling in the regulation of injury-induced axon degeneration (Chen et al., 2012; Xiong and Collins, 2012). In this system, JNK signaling promotes local axon degeneration via the degradation of the survival factors NMNAT2 and SCG10, leading to the depletion of NAD^+ and ATP in injured axons (Shin et al., 2012b; Yang et al., 2015; Walker et al., 2017). By contrast, canonical JNK signaling is also implicated in axon regeneration by activating the downstream nuclear transcription factors, namely AP-

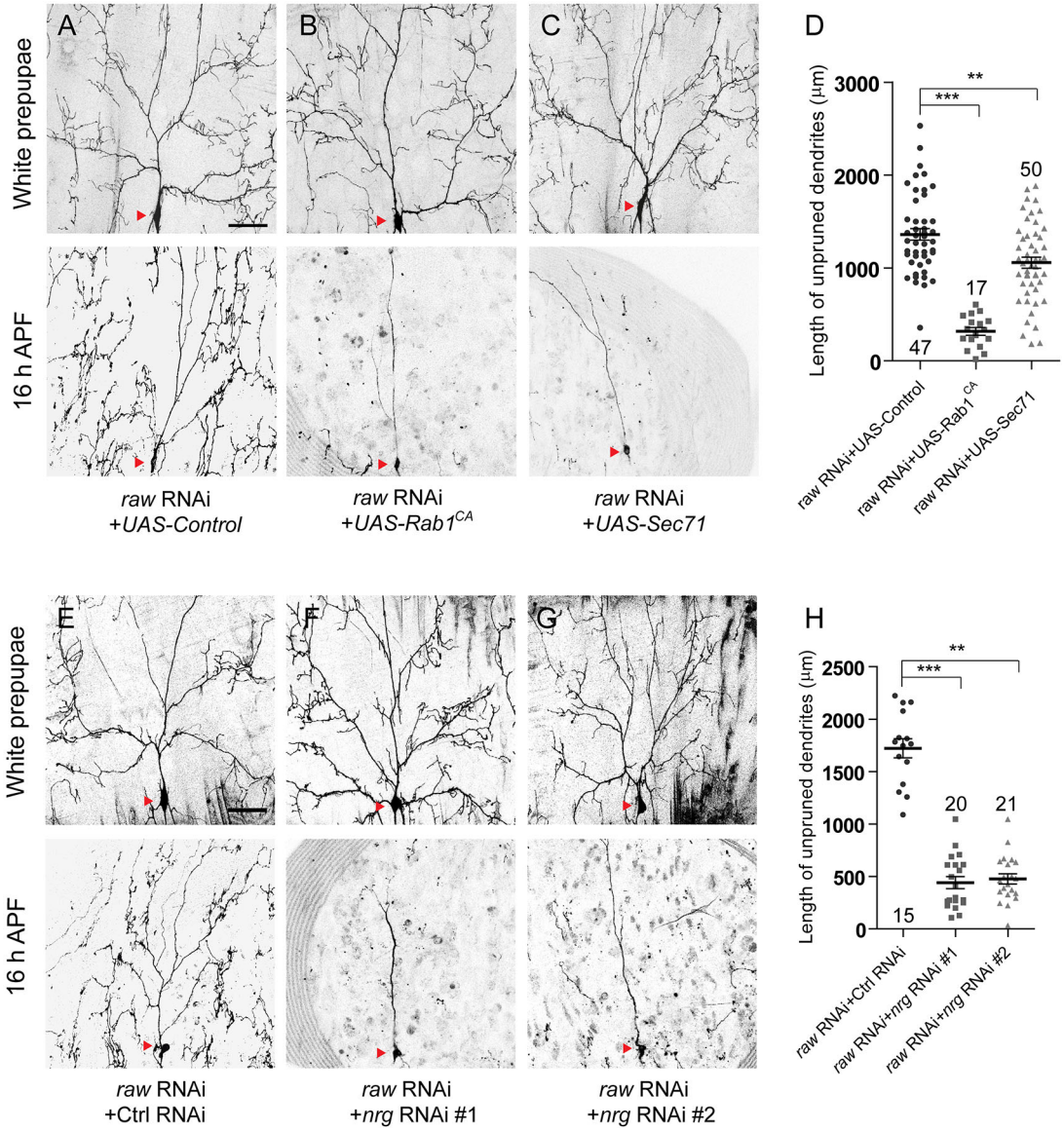

Fig. 7. Raw regulates dendrite pruning partly via the secretory pathway. (A-C,E-G) Live confocal images of ddaC neurons expressing mCD8::GFP driven by *ppk-Gal4* at WP and 16 h APF stages. Dendrites of *raw* RNAi+*UAS-Control* (A), *raw* RNAi+*UAS-Rab1^{CA}* (B), *raw* RNAi+*UAS-Sec71* (C), *raw* RNAi+Ctrl RNAi (E), *raw* RNAi+*nrg* RNAi #1 (F) and *raw* RNAi+*nrg* RNAi #2 (G) ddaC neurons. Red arrowheads indicate the ddaC somas. (D,H) Quantitative analysis of unpruned dendrite lengths. In D,H, data are mean±s.e.m. One-way ANOVA with Bonferroni's test was applied to determine statistical significance. ***P*<0.01; ****P*<0.001. The number of neurons (*n*) examined in each group is shown on the bars. Scale bars: 50 µm.

Development (2020) 147, dev191155. doi:10.1242/dev.191155

1 complex (Xiong et al., 2010; Chen et al., 2012; Shin et al., 2012a). JNK also plays crucial roles in regulating axon pruning of MB γ neurons and dendrite pruning of sensory neurons. JNK signaling acts through a non-canonical mechanism to destabilize the cell-adhesion molecule Fasciclin II and specifically govern axon pruning in MB γ neurons (Bornstein et al., 2015). In contrast, JNK signaling, via the downstream AP-1 transcriptional complex, regulates dendrite pruning of sensory neurons in a canonical manner (Zhu et al., 2019). Moreover, a recent study has reported that Fos and Jun are negatively regulated by Raw to promote degeneration of injured axons in motor neurons (Hao et al., 2019). However, it remains unknown whether this antagonism between Raw and JNK signaling occurs in ddaC sensory neurons prior to dendrite pruning and whether it is required for dendrite pruning.

In this study, we show that Raw regulates dendrite pruning of ddaC neurons in a JNK-independent manner. The antagonism between Raw and JNK signaling takes place in ddaC sensory neurons prior to dendrite pruning. However, interestingly, we show that this antagonism is dispensable for dendrite pruning. We found that loss of *raw* function led to an increase in the expression of the JNK reporter *puc-LacZ* at WP stage, suggesting elevated JNK signaling. However, this elevated JNK signaling is not required for the dendrite pruning defects in *raw* RNAi or mutant ddaC neurons. First, overexpression of either JNK^{DN} constructs, which blocked *puc-lacZ* upregulation, did not rescue the dendrite pruning defects in *raw* RNAi or $raw^{155.27}$ mutant neurons. Second, the treatment of the DLK inhibitor GNE-3511, which abolished the induction of *puc-lacZ*, was not able to rescue the dendrite pruning defects in *raw* RNAi neurons. Third, overexpression of JNK, Fos or Jun did not cause the dendrite pruning defects. Finally, overexpression of Fos^{DN} or Jun^{DN}, the dominant-negative forms of two JNK downstream effectors Fos and Jun, failed to rescue the *raw* RNAi phenotypes. In contrast, Fos^{DN} or Jun^{DN} overexpression has been reported to significantly rescue injury-induced axon degeneration in the *raw* mutant motor neurons (Hao et al., 2019). Thus, we provide multiple lines of evidence demonstrating that Raw regulates dendrite pruning independently of the JNK signaling via an unknown mechanism.

Raw modulates the secretory pathway during dendrite pruning

We have previously reported that the cell-adhesion molecule Nrg is internalized from the plasma membrane to early endosomes and drastically downregulated by the endolysosomal pathway to trigger dendrite pruning (Zhang et al., 2014). Raw was shown to distribute in both membranes and cytoplasm; at least some of the protein could be targeted to the plasma membrane to regulate terminal dendrite branching as a cell-adhesion molecule in C4da neurons (Lee et al., 2015). However, unlike Nrg, Raw is unlikely degraded by the endolysosomal machinery. First, Raw-RFP did not accumulate on aberrant endosomes in $Rab5^{DN}$- or $Vps4^{DN}$-expressing neurons, in contrast to robust Nrg aggregates in those mutant neurons. Second, in the wild-type neurons, Raw-RFP did not colocalize with GFP-2XFYVE-positive early endosomes before the onset of dendrite pruning, whereas Nrg was drastically redistributed from the plasma membrane to the endosomes. Finally, overexpression of Raw did not protect the dendrites from pruning, which differs from a protective role of Nrg overexpression in dendrite pruning. Thus, Raw is unlikely to regulate dendrite pruning via a cell-adhesion mechanism.

How does Raw regulate dendrite pruning of ddaC neurons during early metamorphosis? Raw can regulate dendrite patterning in part by activating the Trc/Fry pathway (Lee et al., 2015). However, this mechanism appears to be dispensable for dendrite pruning, as no dendrite pruning defect was observed in mutant neurons devoid of Trc or its interacting protein Fry. Given that Raw regulates cadherin-based adhesion by localizing β-catenin to the cell surface during gonad development (Jemc et al., 2012), we explored a potential role of Raw in the distribution of the cell-adhesion molecule Nrg in dendrite pruning. Interestingly, we found that loss of *raw* function caused robust accumulation of Nrg in ddaC neurons, suggesting that Raw promotes endolysosmal degradation of Nrg before dendrite pruning. Moreover, loss or reduction of *raw* function did not lead to accumulation of ubiquitylated protein aggregates or the presence of enlarged endosomes, in contrast to *rab5* or *vps4* mutants, suggesting that Raw may indirectly regulate the Rab5/ESCRT-dependent endolysosomal pathway. We realized that the *raw* phenotypes mimic those in mutant neurons devoid of secretory regulators, including Arf1/Sec71 and Rab1/Sar1 (Wang et al., 2017, 2018). Thus, these findings lead us to pinpoint a novel role for Raw in regulating the secretory pathway to promote Nrg downregulation and dendrite pruning. First, loss of *raw* function led to significant decreases in the levels of various ER/Golgi markers, as well as impaired protein secretion. However, the larger number of smaller ER/Golgi puncta were still present in the soma of *raw* RNAi neurons, in contrast to a loss of ER/Golgi punctate signals in *arf1* or *sec71* mutant neurons (Wang et al., 2017), suggesting that Raw may function as an auxiliary regulator to modulate efficient protein secretion. In line with this idea, Raw-RFP appears to colocalize with some of the KDEL-GFP-positive ER compartments and localizes adjacent to GalT-GFP-positive Golgi compartments. In contrast, Arf1/Sec71 and Yif1/Yip likely act as core components of the secretory organelles to fully colocalize with *trans*-Golgi and *cis*-Golgi (Wang et al., 2017, 2018), respectively. Thus, our data suggest that Raw is unlikely a core component of ER/Golgi organelles but might regulate some vesicular sub-compartment of the secretory pathway. Raw protein was also shown to be integrated to the plasma membrane to in C4da neurons (Lee et al., 2015). Thus, our observations imply that Raw might shuttle between secretory vesicles and plasma membrane. Finally, elevated secretory pathway, via $Rab1^{CA}$ or Sec71 overexpression, significantly restored Nrg expression to the normal level and rescued the dendrite pruning defects in *raw* RNAi neurons. Thus, our study provides multiple lines of evidence showing that Raw regulates Nrg degradation and dendrite pruning via the modulation of the secretory pathway. Nrg is a key cell-adhesion molecule that promotes dendrite arborization and mediates dendrite-epidermis interactions during larval growth stages (Yang et al., 2011; Yang et al., 2019). At the onset of dendrite pruning, the secretory pathway might be required to specifically secrete an unknown ligand to trigger the endocytosis of Nrg; alternatively, it may maintain the proper bending rigidity of the plasma membrane, which is important for endocytosis of Nrg. Therefore, disruption of the secretory pathway may result in the retention of Nrg on dendritic plasma membrane and thereby inhibition of dendrite pruning.

Raw and its nematode ortholog OLRN-1 play important roles in neuronal fate, dendrite branching and pruning (this study) (Bauer Huang et al., 2007; Lee et al., 2015). Although Raw has no obvious counterpart in mammals, its N-terminal region bears some homology to mucins and leucine-rich repeat proteins (Lee et al., 2015). Moreover, the secretory regulators and Nrg are highly conserved in vertebrates, and their mammalian orthologs are essential for dendrite growth and neuronal morphogenesis in various developmental contexts (Kenwrick et al., 2000; Horton and Ehlers, 2003, 2004; Horton et al., 2005; Godenschwege et al., 2006; Maness and Schachner, 2007). Thus, the JNK-independent role of *Drosophila*

Development (2020) 147, dev191155. doi:10.1242/dev.191155

Raw in the secretory pathway and neuronal remodeling might be conserved during neuronal pruning and remodeling in vertebrates.

MATERIALS AND METHODS

Fly strains

Fly strains used were: *UAS-mical^{NT}* (Terman et al., 2002), *ppk-Gal4* on II and III chromosome (Grueber et al., 2003), *SOP-flp (#42)* (Matsubara et al., 2011), *UAS-EB1-GFP* (Stone et al., 2008), *raw$^{134.47}$*, *raw$^{155.27}$* (Jemc et al., 2012), *puc*-lacZ (Martin-Blanco et al., 1998), *UAS-Rab5^{DN}*, *UAS-GFP-2xFYVE* (Wucherpfennig et al., 2003), *UAS-Vps4^{DN}* (Rusten et al., 2007), *UAS-Jun^{DN}* (Hao et al., 2019), *UAS-Fos^{DN}* (Hao et al., 2019), *UAS-Sec31-mCherry* (Forster et al., 2010), *UAS-Arf6^{CA}* (Dottermusch-Heidel et al., 2012), *UAS-GFP-Raw* (Lee et al., 2015), *UAS-Sar1^{T34N}*, *UAS-Rab1^{CA}*, *UAS-Sec71* (Yu lab) and *A58-Gal4* (Galko and Krasnow, 2004).

The following stocks were obtained from Bloomington Stock Centre (BSC): *UAS mCD8*::GFP, *FRT40A*, *UAS-Dicer2*, *tubP-Gal80*, *elav-Gal4^{C155}* (BL#458), *UAS-JNK^{DN} #1* (BL#6409), *UAS-JNK^{DN} #2* (BL#9311), *nrg* RNAi #1 (BL#38215), *nrg* RNAi #2 (BL#37496), *UAS-ManII-GFP* (BL#65248), *UAS-Rab11^{CA}* (BL#50783), *UAS-GalT-GFP* (BL#30902), *UAS-GalT-RFP* (BL#30907), *UAS-GFP-KDEL* (BL#9899), *UAS-JNK* (BL#6407), *UAS-Fos* (BL#7213), *UAS-Jun* (BL#7216), *raw^{MI07292}* (BL#44702), *GSG2295-Gal4* (BL#40266), *trc^{1}* (BL#5261) and *fry^{1}* (BL#32103).

The following stocks were obtained from the Vienna *Drosophila* RNAi Centre (VDRC): *raw* RNAi (v101255), *arf1* RNAi (v23082) and control RNAi (v36355, v37288).

A complete list of the fly genotypes shown in each figure is provided in the supplementary Materials and Methods.

Generation of various *raw* transgenes

The *raw* full-length cDNA was PCR amplified from the EST clone GH23250 (DGRC) into Topo Entry and pDonor, respectively (Life Tech). The variants of Raw deletions were generated by site mutagenesis (Agilent Technology). The GATEWAY pTW, pTWV or pTWR vectors containing the *raw* cDNA were constructed by LR reaction (Life Tech) and several transgenic lines were established by Bestgene.

Immunohistochemistry and antibodies

The following primary antibodies were used for immunohistochemistry at the indicated dilution: mouse anti-β-galactosidase (1:1000, Promega, Z3781), mouse anti-Nrg (1:20, BP104, DSHB), mouse anti-Futsch (1:50, 22C10, DSHB), guinea pig anti-Arf1 (1:200, F.Y.'s Lab), guinea pig anti-Sec71 (1:200, F.Y.'s Lab), rabbit anti-Rab1 (1:250, Yu Lab), rabbit anti-GM130 (1:200, Abcam, ab52649), mouse anti-Ubiquitin (1:500; FK2, Enzo Life Sciences, BML-PW0150-0100), chicken anti-Avl (1:500; a gift from D. Bilder, University of California, Berkeley, CA, USA), rat monoclonal anti-mCD8 (1:100, Invitrogen, 11-0081-82) and rabbit anti-Ppk26 (1:1000, a gift from Y. N. Jan, University of California San Francisco, CA, USA; and Z. Wang, Institute of Neuroscience, Shanghai, China). Cy3 or Cy5-conjugated secondary antibodies (Jackson Laboratories, 111-165-003 and 112-095-003) were used at 1:500 dilution. For immunostaining, pupae or larvae were dissected in ice-cold PBS and fixed with 4% formaldehyde for 20 min. The control and mutant samples were incubated simultaneously in the same tubes. Mounting was performed in VectaShield mounting medium, and the samples were directly visualized using an Olympus FV3000 confocal microscope.

Live imaging analysis

To image the dendrites of da sensory neurons at WP stage, pupae were collected and briefly washed with PBS buffer, followed by immersion with 90% glycerol. To image da neurons at 16 h APF or 19 h APF, pupal cases were carefully removed before mounted with 90% glycerol. Dendrite arbors were imaged by using the Leica TSC SP2 confocal microscopy.

Live-imaging of EB1-GFP comet

Larvae (96 h AEL) were immersed in a drop of halocarbon oil (Santa Cruz Biotechnology, sc-250077) and mounted onto slides for time-lapse imaging. Time-lapse imaging was carried out to record EB1-GFP comets with an Olympus FV3000 using a 60× oil lens with 3× zoom. Eighty-three frames were acquired at 2.25 s intervals with six *z*-steps. Kymographs were generated for *z*-projected time-lapse images using the Kymographbuilder plug-in in ImageJ.

Brain protein extraction for co-immunoprecipitation

Adult flies were collected and decapitated by vigorous shaking after frozen. The lysis buffer (Pierce, 87788) was freshly mixed with the protease inhibitor (Roche, Cat#11697498001) to extract proteins from the fly heads. Venus-tagged Raw protein was immunoprecipitated with anti-GFP beads (Chromotek, GFP-Trap A), and subjected to standard western blot analyses. Each co-immunoprecipitation assay was repeated three times.

MARCM analysis of da sensory neurons

We carried out MARCM clonal analysis, dendrite imaging and branch quantification as previously described (Kirilly et al., 2009). ddaC or da clones were chosen and imaged according to their location and morphology at the WP stage. ddaC neurons were examined for dendrite pruning defects at 16 h or 19 h APF.

RU486/mifepristone treatment and trafficking assay

RU486/mifepristone treatment was performed as previously described (Wang et al., 2017). Embryos were collected at 6 h intervals and cultivated on standard food to the early 3rd instar larva stage. Subsequently, the larvae grew in the standard culture medium with 240 µg/ml mifepristone (Sigma-Aldrich, M8046) for 24 h. wL3 larvae were picked and dissected in PBS and fixed with 4% formaldehyde for 20 min. The fillets were incubated with rat monoclonal anti-CD8α in PBS and washed three times with PBS in the detergent-free condition, which was followed by Cy3-conjugated secondary antibody incubation and washed three times in the detergent-free condition. The intensity of immunofluorescence was measured in the same confocal setting for both mutant and control neurons.

GNE-3511 treatment

Embryos were collected at 12 h intervals and reared on the standard food. The larvae were then transferred to the food containing 50 µM GNE-3511 (Millipore, 5.33168.0001). Wandering 3rd instar larvae were collected after 1-2 days of drug feeding and used for anti-β-gal staining at WP stage. WPs were collected after 1-2 days of drug feeding and used for testing dendrite pruning at 16 h APF.

Quantification of dendrites

Live confocal images of da neurons expressing UAS-mCD8-GFP were performed at WP, 16 h and 19 h APF stages. Dorsal is upwards in all images. The percentage of severing defects is the percentage of ddaC neurons with larval dendrites attached to the soma at 16 h APF. The length of unpruned dendrites was measured in a 275 µm×275 µm region derived from the dorsal dendritic field of ddaC neurons, ranging from the abdominal segments 2-4. The number of neurons (*n*) examined in each group is shown on the bars. Plots of average length and s.e.m. were generated using GraphPad Prism software.

Quantification of immunostaining

Images were obtained from projected *z*-stacks (at 1.5 µm intervals) to cover the entire volume of da sensory neurons using an Olympus FV3000 confocal microscope. To measure the fluorescence intensities, cell nuclei (*puc-lacZ* immunostaining) or whole soma (Nrg/Arf1/Rab1/Sec71/GM130 immunostaining and Sec31-mCherry/GalT-RFP live imaging) contours were drawn on the appropriate fluorescent channel based on the GFP channel in ImageJ software. After subtracting the background (Rolling Ball Radius=30) from the entire image of that channel, we measured the mean gray value in the marked area in ddaC and/or ddaE on the same images and calculated their ratios. The ratios were normalized to the corresponding average control values and subjected to statistical analysis for comparison between different conditions. Graphs display the average values of the ddaC/ddaE ratios and the s.e.m. normalized to controls. The number of ddaC neurons (*n*) examined in each group is shown on the bars. Insets show the

ddaC neurons labeled by *ppk-Gal4*-driven mCD8-GFP expression. The number of ddaC neurons (*n*) examined in each group is shown on the bars. Dorsal is upwards in all images.

To quantify the alterations of dendritic Fustch and mCD8-GFP distribution, we measured their intensities in the 20 µm of major dorsal dendrites that were 30 µm away from the soma. The number of ddaC neurons (*n*) examined in each group is shown on the bars. Dorsal is upwards in all images.

Statistics

For pairwise comparison, two-tailed Student's *t*-test was used to determine statistical significance. For multiple-group comparison, one-way ANOVA with Bonferroni's test was used to determine significance. Error bars in all graphs represent s.e.m. Statistical significance was defined as ****$P<0.0001$, ***$P<0.001$, **$P<0.01$, *$P<0.05$ and n.s., not significant. The number of neurons (*n*) in each group is shown on the bars.

Acknowledgements

We thank H. Bellen, D. Bilder, E. H. Chen, C. A. Collins, M. V. Doren, M. Gonzalez-Gaitan, Y. Jan, A. L. Kolodkin, S. Luschig, S. F. Onel, J. Z. Parrish, J. Pielage, M. M. Rolls, H. Stenmark, T. Uemura, the Bloomington Stock Center (BSC), DSHB (University of Iowa) and VDRC (Austria) for generously providing antibodies and fly stocks. We thank Yu lab members for helpful discussion and assistance.

Competing interests

The authors declare no competing or financial interests.

Author contributions

Conceptualization: F.Y.; Methodology: M.R., L.Y.C.; Validation: M.R., F.Y.; Formal analysis: M.R., S.B., L.Y.C., Q.W., F.Y.; Investigation: M.R., S.B., L.Y.C., Q.W., F.Y.; Resources: M.R., S.B., Q.W.; Data curation: M.R.; Writing - original draft: M.R., F.Y.; Writing - review & editing: F.Y.; Visualization: M.R., S.B., L.Y.C., Q.W.; Supervision: F.Y.; Project administration: F.Y.; Funding acquisition: F.Y.

Funding

This work was funded by the Temasek Life Sciences Laboratory Singapore (TLL-2040) and by the National Research Foundation Singapore (SBP-P3 and SBP-P8) (both to F.Y.).

Supplementary information

Supplementary information available online at
https://dev.biologists.org/lookup/doi/10.1242/dev.191155.supplemental

Peer review history

The peer review history is available online at
https://dev.biologists.org/lookup/doi/10.1242/dev.191155.reviewer-comments.pdf

References

Bagri, A., Cheng, H.-J., Yaron, A., Pleasure, S. J. and Tessier-Lavigne, M. (2003). Stereotyped pruning of long hippocampal axon branches triggered by retraction inducers of the semaphorin family. *Cell* **113**, 285-299. doi:10.1016/S0092-8674(03)00267-8

Bates, K. L., Higley, M. and Letsou, A. (2008). Raw mediates antagonism of AP-1 activity in Drosophila. *Genetics* **178**, 1989-2002. doi:10.1534/genetics.107.086298

Bauer Huang, S. L., Saheki, Y., VanHoven, M. K., Torayama, I., Ishihara, T., Katsura, I., van der Linden, A., Sengupta, P. and Bargmann, C. I. (2007). Left-right olfactory asymmetry results from antagonistic functions of voltage-activated calcium channels and the Raw repeat protein OLRN-1 in C. elegans. *Neural Dev.* **2**, 24. doi:10.1186/1749-8104-2-24

Bornstein, B., Zahavi, E. E., Gelley, S., Zoosman, M., Yaniv, S. P., Fuchs, O., Porat, Z., Perlson, E. and Schuldiner, O. (2015). Developmental axon pruning requires destabilization of cell adhesion by JNK signaling. *Neuron* **88**, 926-940. doi:10.1016/j.neuron.2015.10.023

Byars, C. L., Bates, K. L. and Letsou, A. (1999). The dorsal-open group gene raw is required for restricted DJNK signaling during closure. *Development* **126**, 4913-4923.

Chen, L., Stone, M. C., Tao, J. and Rolls, M. M. (2012). Axon injury and stress trigger a microtubule-based neuroprotective pathway. *Proc. Natl. Acad. Sci. USA* **109**, 11842-11847. doi:10.1073/pnas.1121180109

Coffey, E. T. (2014). Nuclear and cytosolic JNK signalling in neurons. *Nat. Rev. Neurosci.* **15**, 285-299. doi:10.1038/nrn3729

Dottermusch-Heidel, C., Groth, V., Beck, L. and Önel, S.-F. (2012). The Arf-GEF Schizo/Loner regulates N-cadherin to induce fusion competence of Drosophila myoblasts. *Dev. Biol.* **368**, 18-27. doi:10.1016/j.ydbio.2012.04.031

Feng, C., Thyagarajan, P., Shorey, M., Seebold, D. Y., Weiner, A. T., Albertson, R. M., Rao, K. S., Sagasti, A., Goetschius, D. J. and Rolls, M. M. (2019). Patronin-mediated minus end growth is required for dendritic microtubule polarity. *J. Cell Biol.* **218**, 2309-2328. doi:10.1083/jcb.201810155

Förster, D., Armbruster, K. and Luschnig, S. (2010). Sec24-dependent secretion drives cell-autonomous expansion of tracheal tubes in Drosophila. *Curr. Biol.* **20**, 62-68. doi:10.1016/j.cub.2009.11.062

Galko, M. J. and Krasnow, M. A. (2004). Cellular and genetic analysis of wound healing in Drosophila larvae. *PLoS Biol.* **2**, e239. doi:10.1371/journal.pbio.0020239

Godenschwege, T. A., Kristiansen, L. V., Uthaman, S. B., Hortsch, M. and Murphey, R. K. (2006). A conserved role for Drosophila Neuroglian and human L1-CAM in central-synapse formation. *Curr. Biol.* **16**, 12-23. doi:10.1016/j.cub.2005.11.062

Grueber, W. B., Ye, B., Moore, A. W., Jan, L. Y. and Jan, Y. N. (2003). Dendrites of distinct classes of Drosophila sensory neurons show different capacities for homotypic repulsion. *Curr. Biol.* **13**, 618-626. doi:10.1016/S0960-9822(03)00207-0

Han, C., Song, Y., Xiao, H., Wang, D., Franc, N. C., Jan, L. Y. and Jan, Y.-N. (2014). Epidermal cells are the primary phagocytes in the fragmentation and clearance of degenerating dendrites in Drosophila. *Neuron* **81**, 544-560. doi:10.1016/j.neuron.2013.11.021

Hans, V. R., Wendt, T. I., Patel, A. M., Patel, M. M., Perez, L., Talbot, D. E. and Jemc, J. C. (2018). Raw regulates glial population of the eye imaginal disc. *Genesis* **56**, e23254. doi:10.1002/dvg.23254

Hao, Y., Waller, T. J., Nye, D. M., Li, J., Zhang, Y., Hume, R. I., Rolls, M. M. and Collins, C. A. (2019). Degeneration of injured axons and dendrites requires restraint of a protective jnk signaling pathway by the transmembrane protein raw. *J. Neurosci.* **39**, 8457-8470. doi:10.1523/JNEUROSCI.0016-19.2019

Herzmann, S., Krumkamp, R., Rode, S., Kintrup, C. and Rumpf, S. (2017). PAR-1 promotes microtubule breakdown during dendrite pruning in Drosophila. *EMBO J.* **36**, 1981-1991. doi:10.15252/embj.201695890

Herzmann, S., Gotzelmann, I., Reekers, L. F. and Rumpf, S. (2018). Spatial regulation of microtubule disruption during dendrite pruning in Drosophila. *Development* **145**, dev156950. doi:10.1242/dev.156950

Horton, A. C. and Ehlers, M. D. (2003). Neuronal polarity and trafficking. *Neuron* **40**, 277-295. doi:10.1016/S0896-6273(03)00629-9

Horton, A. C. and Ehlers, M. D. (2004). Secretory trafficking in neuronal dendrites. *Nat. Cell Biol.* **6**, 585-591. doi:10.1038/ncb0704-585

Horton, A. C., Rácz, B., Monson, E. E., Lin, A. L., Weinberg, R. J. and Ehlers, M. D. (2005). Polarized secretory trafficking directs cargo for asymmetric dendrite growth and morphogenesis. *Neuron* **48**, 757-771. doi:10.1016/j.neuron.2005.11.005

Jan, Y.-N. and Jan, L. Y. (2010). Branching out: mechanisms of dendritic arborization. *Nat. Rev. Neurosci.* **11**, 316-328. doi:10.1038/nrn2836

Jemc, J. C., Milutinovich, A. B., Weyers, J. J., Takeda, Y. and Van Doren, M. (2012). raw Functions through JNK signaling and cadherin-based adhesion to regulate Drosophila gonad morphogenesis. *Dev. Biol.* **367**, 114-125. doi:10.1016/j.ydbio.2012.04.027

Kanamori, T., Togashi, K., Koizumi, H. and Emoto, K. (2015a). Dendritic Remodeling: Lessons from Invertebrate Model Systems. *Int. Rev. Cell Mol. Biol.* **318**, 1-25. doi:10.1016/bs.ircmb.2015.05.001

Kanamori, T., Yoshino, J., Yasunaga, K., Dairyo, Y. and Emoto, K. (2015b). Local endocytosis triggers dendritic thinning and pruning in Drosophila sensory neurons. *Nat. Commun.* **6**, 6515. doi:10.1038/ncomms7515

Kenwrick, S., Watkins, A. and De Angelis, E. (2000). Neural cell recognition molecule L1: relating biological complexity to human disease mutations. *Hum. Mol. Genet.* **9**, 879-886. doi:10.1093/hmg/9.6.879

Kirilly, D., Gu, Y., Huang, Y., Wu, Z., Bashirullah, A., Low, B. C., Kolodkin, A. L., Wang, H. and Yu, F. (2009). A genetic pathway composed of Sox14 and Mical governs severing of dendrites during pruning. *Nat. Neurosci.* **12**, 1497-1505. doi:10.1038/nn.2415

Kirilly, D., Wong, J. J., Lim, E. K., Wang, Y., Zhang, H., Wang, C., Liao, Q., Wang, H., Liou, Y.-C. and Yu, F. (2011). Intrinsic epigenetic factors cooperate with the steroid hormone ecdysone to govern dendrite pruning in Drosophila. *Neuron* **72**, 86-100. doi:10.1016/j.neuron.2011.08.003

Krämer, R., Rode, S. and Rumpf, S. (2019). Rab11 is required for neurite pruning and developmental membrane protein degradation in Drosophila sensory neurons. *Dev. Biol.* **451**, 68-78. doi:10.1016/j.ydbio.2019.03.003

Kuo, C. T., Jan, L. Y. and Jan, Y. N. (2005). Dendrite-specific remodeling of Drosophila sensory neurons requires matrix metalloproteases, ubiquitin-proteasome, and ecdysone signaling. *Proc. Natl. Acad. Sci. USA* **102**, 15230-15235. doi:10.1073/pnas.0507393102

Lee, H.-H., Jan, L. Y. and Jan, Y.-N. (2009). Drosophila IKK-related kinase Ik2 and Katanin p60-like 1 regulate dendrite pruning of sensory neuron during metamorphosis. *Proc. Natl. Acad. Sci. USA* **106**, 6363-6368. doi:10.1073/pnas.0902051106

Lee, J., Peng, Y., Lin, W.-Y. and Parrish, J. Z. (2015). Coordinate control of terminal dendrite patterning and dynamics by the membrane protein Raw. *Development* **142**, 162-173. doi:10.1242/dev.113423
Loncle, N. and Williams, D. W. (2012). An interaction screen identifies headcase as a regulator of large-scale pruning. *J. Neurosci.* **32**, 17086-17096. doi:10.1523/JNEUROSCI.1391-12.2012
Luo, L. and O'Leary, D. D. (2005). Axon retraction and degeneration in development and disease. *Annu. Rev. Neurosci.* **28**, 127-156. doi:10.1146/annurev.neuro.28.061604.135632
Luong, D., Perez, L. and Jemc, J. C. (2018). Identification of raw as a regulator of glial development. *PLoS ONE* **13**, e0198161. doi:10.1371/journal.pone.0198161
Malun, D. and Brunjes, P. C. (1996). Development of olfactory glomeruli: temporal and spatial interactions between olfactory receptor axons and mitral cells in opossums and rats. *J. Comp. Neurol.* **368**, 1-16. doi:10.1002/(SICI)1096-9861(19960422)368:1<1::AID-CNE1>3.0.CO;2-7
Maness, P. F. and Schachner, M. (2007). Neural recognition molecules of the immunoglobulin superfamily: signaling transducers of axon guidance and neuronal migration. *Nat. Neurosci.* **10**, 19-26. doi:10.1038/nn1827
Martin-Blanco, E., Gampel, A., Ring, J., Virdee, K., Kirov, N., Tolkovsky, A. M. and Martinez-Arias, A. (1998). puckered encodes a phosphatase that mediates a feedback loop regulating JNK activity during dorsal closure in Drosophila. *Genes Dev.* **12**, 557-570. doi:10.1101/gad.12.4.557
Matsubara, D., Horiuchi, S.-Y., Shimono, K., Usui, T. and Uemura, T. (2011). The seven-pass transmembrane cadherin Flamingo controls dendritic self-avoidance via its binding to a LIM domain protein, Espinas, in Drosophila sensory neurons. *Genes Dev.* **25**, 1982-1996. doi:10.1101/gad.16531611
Miller, B. R., Press, C., Daniels, R. W., Sasaki, Y., Milbrandt, J. and DiAntonio, A. (2009). A dual leucine kinase-dependent axon self-destruction program promotes Wallerian degeneration. *Nat. Neurosci.* **12**, 387-389. doi:10.1038/nn.2290
O'Leary, D. D. M. and Koester, S. E. (1993). Development of projection neuron types, axon pathways, and patterned connections of the mammalian cortex. *Neuron* **10**, 991-1006. doi:10.1016/0896-6273(93)90049-W
Osterwalder, T., Yoon, K. S., White, B. H. and Keshishian, H. (2001). A conditional tissue-specific transgene expression system using inducible GAL4. *Proc. Natl. Acad. Sci. USA* **98**, 12596-12601. doi:10.1073/pnas.221303298
Riccomagno, M. M. and Kolodkin, A. L. (2015). Sculpting neural circuits by axon and dendrite pruning. *Annu. Rev. Cell Dev. Biol.* **31**, 779-805. doi:10.1146/annurev-cellbio-100913-013038
Riccomagno, M. M., Hurtado, A., Wang, H., Macopson, J. G., Griner, E. M., Betz, A., Brose, N., Kazanietz, M. G. and Kolodkin, A. L. (2012). The RacGAP β2-Chimaerin selectively mediates axonal pruning in the hippocampus. *Cell* **149**, 1594-1606. doi:10.1016/j.cell.2012.05.018
Rui, M., Ng, K. S., Tang, Q., Bu, S. and Yu, F. (2020). Protein phosphatase PP2A regulates microtubule orientation and dendrite pruning in Drosophila. *EMBO Rep.* **21**, e48843. doi:10.15252/embr.201948843
Rumpf, S., Lee, S. B., Jan, L. Y. and Jan, Y. N. (2011). Neuronal remodeling and apoptosis require VCP-dependent degradation of the apoptosis inhibitor DIAP1. *Development* **138**, 1153-1160. doi:10.1242/dev.062703
Rusten, T. E., Vaccari, T., Lindmo, K., Rodahl, L. M., Nezis, I. P., Sem-Jacobsen, C., Wendler, F., Vincent, J.-P., Brech, A., Bilder, D. et al. (2007). ESCRTs and Fab1 regulate distinct steps of autophagy. *Curr. Biol.* **17**, 1817-1825. doi:10.1016/j.cub.2007.09.032
Schuldiner, O. and Yaron, A. (2015). Mechanisms of developmental neurite pruning. *Cell. Mol. Life Sci.* **72**, 101-119. doi:10.1007/s00018-014-1729-6
Sekar, A., Bialas, A. R., de Rivera, H., Davis, A., Hammond, T. R., Kamitaki, N., Tooley, K., Presumey, J., Baum, M., Van Doren, V. et al. (2016). Schizophrenia risk from complex variation of complement component 4. *Nature* **530**, 177-183. doi:10.1038/nature16549
Shin, J. E., Cho, Y., Beirowski, B., Milbrandt, J., Cavalli, V. and DiAntonio, A. (2012a). Dual leucine zipper kinase is required for retrograde injury signaling and axonal regeneration. *Neuron* **74**, 1015-1022. doi:10.1016/j.neuron.2012.04.028
Shin, J. E., Miller, B. R., Babetto, E., Cho, Y., Sasaki, Y., Qayum, S., Russler, E. V., Cavalli, V., Milbrandt, J. and DiAntonio, A. (2012b). SCG10 is a JNK target in the axonal degeneration pathway. *Proc. Natl. Acad. Sci. USA* **109**, E3696-E3705. doi:10.1073/pnas.1216204109
Stone, M. C., Roegiers, F. and Rolls, M. M. (2008). Microtubules have opposite orientation in axons and dendrites of Drosophila neurons. *Mol. Biol. Cell* **19**, 4122-4129. doi:10.1091/mbc.e07-10-1079
Tang, G., Gudsnuk, K., Kuo, S.-H., Cotrina, M. L., Rosoklija, G., Sosunov, A., Sonders, M. S., Kanter, E., Castagna, C., Yamamoto, A. et al. (2014). Loss of mTOR-dependent macroautophagy causes autistic-like synaptic pruning deficits. *Neuron* **83**, 1131-1143. doi:10.1016/j.neuron.2014.07.040
Tang, Q., Rui, M., Bu, S., Wang, Y., Chew, L. Y. and Yu, F. (2020). A microtubule polymerase is required for microtubule orientation and dendrite pruning in Drosophila. *EMBO J.* **39**, e103549. doi:10.15252/embj.2019103549
Tapia, J. C., Wylie, J. D., Kasthuri, N., Hayworth, K. J., Schalek, R., Berger, D. R., Guatimosim, C., Seung, H. S. and Lichtman, J. W. (2012). Pervasive synaptic branch removal in the mammalian neuromuscular system at birth. *Neuron* **74**, 816-829. doi:10.1016/j.neuron.2012.04.017
Terman, J. R., Mao, T., Pasterkamp, R. J., Yu, H.-H. and Kolodkin, A. L. (2002). MICALs, a family of conserved flavoprotein oxidoreductases, function in plexin-mediated axonal repulsion. *Cell* **109**, 887-900. doi:10.1016/S0092-8674(02)00794-8
Truman, J. W. (1990). Metamorphosis of the central nervous system of Drosophila. *J. Neurobiol.* **21**, 1072-1084. doi:10.1002/neu.480210711
Walker, L. J., Summers, D. W., Sasaki, Y., Brace, E. J., Milbrandt, J. and DiAntonio, A. (2017). MAPK signaling promotes axonal degeneration by speeding the turnover of the axonal maintenance factor NMNAT2. *Elife* **6**, e22540. doi:10.7554/eLife.22540
Wang, Y., Zhang, H., Shi, M., Liou, Y.-C., Lu, L. and Yu, F. (2017). Sec71 functions as a GEF for the small GTPase Arf1 to govern dendrite pruning of Drosophila sensory neurons. *Development* **144**, 1851-1862. doi:10.1242/dev.146175
Wang, Q., Wang, Y. and Yu, F. (2018). Yif1 associates with Yip1 on Golgi and regulates dendrite pruning in sensory neurons during Drosophila metamorphosis. *Development* **145**, dev164475. doi:10.1242/dev.164475
Wang, Y., Rui, M., Tang, Q., Bu, S. and Yu, F. (2019). Patronin governs minus-end-out orientation of dendritic microtubules to promote dendrite pruning in Drosophila. *Elife* **8**, e39964. doi:10.7554/eLife.39964.041
Williams, D. W. and Truman, J. W. (2005). Cellular mechanisms of dendrite pruning in Drosophila: insights from in vivo time-lapse of remodeling dendritic arborizing sensory neurons. *Development* **132**, 3631-3642. doi:10.1242/dev.01928
Williams, D. W., Kondo, S., Krzyzanowska, A., Hiromi, Y. and Truman, J. W. (2006). Local caspase activity directs engulfment of dendrites during pruning. *Nat. Neurosci.* **9**, 1234-1236. doi:10.1038/nn1774
Wong, J. J. L., Li, S., Lim, E. K. H., Wang, Y., Wang, C., Zhang, H., Kirilly, D., Wu, C., Liou, Y.-C., Wang, H. et al. (2013). A Cullin1-based SCF E3 ubiquitin ligase targets the InR/PI3K/TOR pathway to regulate neuronal pruning. *PLoS Biol.* **11**, e1001657. doi:10.1371/journal.pbio.1001657
Wucherpfennig, T., Wilsch-Brauninger, M. and González-Gaitán, M. (2003). Role of Drosophila Rab5 during endosomal trafficking at the synapse and evoked neurotransmitter release. *J. Cell Biol.* **161**, 609-624. doi:10.1083/jcb.200211087
Xiong, X. and Collins, C. A. (2012). A conditioning lesion protects axons from degeneration via the Wallenda/DLK MAP kinase signaling cascade. *J. Neurosci.* **32**, 610-615. doi:10.1523/JNEUROSCI.3586-11.2012
Xiong, X., Wang, X., Ewanek, R., Bhat, P., Diantonio, A. and Collins, C. A. (2010). Protein turnover of the Wallenda/DLK kinase regulates a retrograde response to axonal injury. *J. Cell Biol.* **191**, 211-223. doi:10.1083/jcb.201006039
Yang, W.-K., Peng, Y.-H., Li, H., Lin, H.-C., Lin, Y.-C., Lai, T.-T., Suo, H., Wang, C.-H., Lin, W.-H., Ou, C.-Y. et al. (2011). Nak regulates localization of clathrin sites in higher-order dendrites to promote local dendrite growth. *Neuron* **72**, 285-299. doi:10.1016/j.neuron.2011.08.028
Yang, J., Wu, Z., Renier, N., Simon, D. J., Uryu, K., Park, D. S., Greer, P. A., Tournier, C., Davis, R. J. and Tessier-Lavigne, M. (2015). Pathological axonal death through a MAPK cascade that triggers a local energy deficit. *Cell* **160**, 161-176. doi:10.1016/j.cell.2014.11.053
Yang, W. K., Chueh, Y. R., Cheng, Y. J., Siegenthaler, D., Pielage, J. and Chien, C. T. (2019). Epidermis-derived L1CAM homolog neuroglian mediates dendrite enclosure and blocks heteroneuronal dendrite bundling. *Curr. Biol.* **29**, 1445-1459.e3. doi:10.1016/j.cub.2019.03.050
Yu, F. and Schuldiner, O. (2014). Axon and dendrite pruning in Drosophila. *Curr. Opin. Neurobiol.* **27**, 192-198. doi:10.1016/j.conb.2014.04.005
Zhang, H., Wang, Y., Wong, J. J. L., Lim, K.-L., Liou, Y.-C., Wang, H. and Yu, F. (2014). Endocytic pathways downregulate the L1-type cell adhesion molecule neuroglian to promote dendrite pruning in Drosophila. *Dev. Cell* **30**, 463-478. doi:10.1016/j.devcel.2014.06.014
Zhou, J., Edgar, B. A. and Boutros, M. (2017). ATF3 acts as a rheostat to control JNK signalling during intestinal regeneration. *Nat. Commun.* **8**, 14289. doi:10.1038/ncomms14289
Zhu, S., Chen, R., Soba, P. and Jan, Y. N. (2019). JNK signaling coordinates with ecdysone signaling to promote pruning of Drosophila sensory neuron dendrites. *Development* **146**, dev163592. doi:10.1242/dev.163592